Isolation of SOS2 inhibiting Affimer reagents to study the role of SOS2 in Ras mediated cancer signalling

Keri Marie Fishwick

Submitted in accordance with the requirements for the degree of

Master of Science by Research

The University of Leeds

Faculty of Biological Sciences

School of Molecular and Cellular Biology

June 2020

The candidate confirms that the work submitted is her own and that appropriate credit has been given where reference has been made to the work of others.

Acknowledgements

Thank you to Dr Darren Tomlinson for allowing me to complete my master's within the lab. I have learnt a lot and know it will put me in good stead for the future.

Thank you to everyone within the Tomlinson lab for all their help throughout my time in the lab. Specifically, thanks to Sophie Saunders for teaching me protein production, the nucleotide exchange assay and more, as well as Dr Christian Tiede and Anna Tang for teaching me phage display. It has been a great albeit shortened year, with the recent addition of frequent Zoom coffee mornings and quizzes really getting me through the past few months of lockdown whilst writing up my thesis.

Abstract

Ras is an important activator of both the MAPK/ERK and PI3K/Akt pathways. It has been found to be mutated in a third of all human cancers, making it an important therapeutic target. Ras has been described as an undruggable target, however, recently compounds have been identified which inhibit Ras function. Another potentially important target in these pathways is SOS, a multidomain guanine exchange factors of Ras. SOS1 is the most studied human isoform of SOS, however, it is important to further understand the role of SOS2 in Ras mediated cancer signalling. Artificial binding proteins, such as Affimers, provide a novel tool to understand the roles of SOS1 and SOS2 in Ras activation both in normal and cancer cells. Previously Affimers have been isolated that inhibit SOS1 and SOS2. Here, Affimer reagents that specifically bind to the catalytic domain of SOS2 were isolated and characterised in nucleotide exchange assays. The Affimer reagents tested so far do not inhibit nucleotide exchange, however, other SOS2 selective Affimer reagents still need to be characterised. Additional biochemical characterisation has also been carried out for a SOS1/SOS2 cross-reactive Affimer reagent, isolated previously. This Affimer reagent inhibits SOS1 with a nanomolar potency, as well as having the ability to inhibit SOS2. Alanine scanning of this Affimer reagent revealed five residues which are important for inhibiting SOS1. These biochemical characterisation techniques can also be applied to SOS2 inhibitors, alongside mammalian cell assays, to study the role of SOS2 in the MAPK/ERK and PI3K/Akt pathways.

Table of Contents

List of Figures

List of Tables

List of Abbreviations

2TY-carb	2TY media containing 100 µg/mL carbenicillin
A_{260} / A_{280} / A_{562} / A_{620}	Absorbance at 260 / 280 / 562 / 620 nm
ANOVA	Analysis of variance
BCA	Bicinchoninic acid
Carb	Carbenicillin
DARPin	Designed Ankyrin Repeat Protein
DH	Dbl-homology
DNA	Deoxyribonucleic acid
DTT	Dithiothreitol
E. coli	*Escherichia coli*
EDTA	Ethylenediaminetetraacetic acid
EGFR	Epidermal growth factor receptor
ELISA	Enzyme-linked immunosorbent assay
ERK	Extracellular signal-regulated kinase
FN3	Fibronectin type III domain
GAB	Grb2-associated binding protein
GAP	GTPase-activating protein
GDP	Guanosine diphosphate
GEF	Guanine Exchange Factor
GF	Growth factor
GFP	Green fluorescent protein
Grb2	Growth factor receptor-bound protein 2
GTP	Guanosine triphosphate
HBC	High binding capacity
HEPES	4-(2-hydroxyethyl)-1-piperazineethanesulfonic acid
HPDP	N-[6-(biotinamido)hexyl]-3'-(2'-pyridyldithio)propionamide
HRP	Horseradish peroxidase
IC_{50}	Half maximal inhibitory concentration
IPTG	Isopropyl β-d-1-thiogalactopyranoside
Kana	Kanamycin
kDa	Kilo-Daltons
KRasmGDP	KRas loaded with mGDP
KRasmGDP-GTP	KRasmGDP in the presence of GTP
LB	Lysogeny broth

MAPK	Mitogen-Activated Protein Kinase
MEF	Mouse embryonic fibroblast
mGDP	Mant-GDP
NES	Nucleotide exchange buffer with SOS and GTP
NHS	N-hydroxysuccinimide
Ni-NTA	Nickel-nitrilotriacetic acid
OD_{600}	Optical density at 600 nm
PA	Phosphatic acid
PBS	Phosphate buffered saline
PBST	PBS with 0.1% Tween-20
PCR	Polymerase chain reaction
PDB	Protein data bank
PDK1	Phosphoinositide-dependent kinase 1
PEG	Polyethylene glycol
pERK	Phosphorylated ERK
PH	Pleckstrin homology
PHLPP	PH domain leucine-rich repeat protein phosphatase
PI3K	Phosphoinositide 3-kinase
PIP2	Phosphatidylinositol 4,5-biphosphate
PIP3	Phosphatidylinositol 3,4,5-triphosphate
PP2A	Protein phosphatase 2
PTEN	Phosphatase and tensing homolog
PxxP	Poly-proline
Rem	Ras exchanger motif
RTK	Receptor tyrosine kinase
SD	Standard deviation
SDS	Sodium dodecyl sulfate
SDS-PAGE	SDS–polyacrylamide gel electrophoresis
SH2	Src homology 2
SH3	Src homology 3
SOS	Son of Sevenless
SOS1-B	Biotinylated $SOS1^{cat}$
$SOS1^{cat}$	Catalytic domain of SOS1
SOS2-B	Biotinylated $SOS2^{cat}$
$SOS2^{cat}$	Catalytic domain of SOS2
TB	Terrific broth

TB-carb	TB autoinduction media containing 100 µg/mL carbenicillin
TBST	Tris-buffered saline with 0.2% Tween-20
TCEP	Tris(2-carboxyethyl)phosphine
TE	Tris-EDTA
TMB	3,3',5,5'-Tetramethylbenzidine
VR	Variable region
WT	Wild-type

1. Introduction

1.1 Ras mediated signalling pathways

Signalling pathways are essential in the coordination of cellular processes, such as cell proliferation, survival and differentiation. Aberrant signalling can be caused by mutations in oncogenes or tumour suppressor genes leading to cancer [1]. For example, mutations in the oncogene Ras is an important step in driving tumour formation and cancer [2]. Two important signalling pathways which can be activated by Ras are the MAPK/ERK pathway and the PI3K/Akt pathway (figure 1).

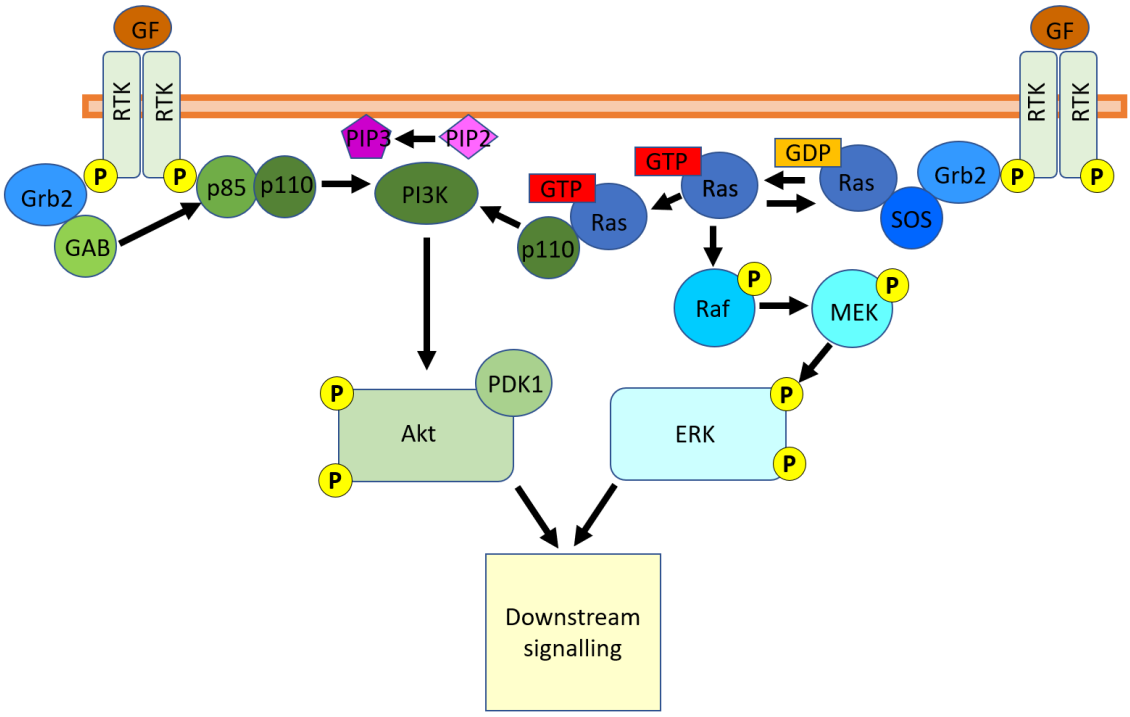

Figure 1: Schematic of the MAPK/ERK and PI3K/Akt pathways. Activation of receptor tyrosine kinases (RTKs) by autophosphorylation following extracellular binding by growth factors (GF) leads to activation of signalling pathways, including the MAPK/ERK pathway (right hand side) and the PI3K/Akt pathway (left hand side).

1.1.1 The MAPK/ERK pathway

The mitogen-activated protein kinase (MAPK) pathways are important examples of signalling pathways that regulate cell proliferation and differentiation, among other processes [3]. The MAPK/ERK pathway is one of the most widely studied. The MAPK/ERK pathway is activated by

a growth factor (GF) binding to the extracellular domain of receptor tyrosine kinases (RTK) [4]. The RTKs may already be in an oligomeric state, or the binding of the GF may induce dimerisation [5]. Upon ligand binding, the tyrosine residues on the intracellular domain of RTKs autophosphorylate, thereby recruiting adapter proteins, such as the growth factor receptor-bound protein 2 (Grb2), via its Src homology 2 (SH2) domain [6]. Grb2 is responsible for the membrane localisation of guanine exchange factors (GEFs), such as Son of Sevenless (SOS), due to its Src homology 3 (SH3) domain binding to C-terminal of SOS [7]. SOS is a positive regulator of Ras and so activates it via facilitating the dissociation of GDP from Ras, allowing GTP to bind in its place [8]. This occurs at the plasma membrane, where Ras is anchored by its post-translational modification of farensylation and a second signal, specific to the Ras isoform [9]. Activation of Ras via binding of GTP allows interaction with the Ras binding domain and cysteine rich domain of the next kinase in the cascade, Raf, which is recruited to the plasma membrane and activated [10]. Activated Raf can then activate MEK via phosphorylation of either serine residue, S217 or S221, on MEK [11]. MEK then activates ERK by phosphorylation of the tyrosine residue and then the threonine residue in the TEY motif (Thr-Glu-Tyr) [12, 13]. Activated ERK causes further downstream signalling by phosphorylating the serine or threonine neighbouring a proline on a substrate, which may be found in the nucleus, cytosol, plasma membrane or cellular organelles [14]. Substrates include the nuclear transcription factors Elk1 and c-Fos, and the cytoplasmic substrate PLA2 [14].

To switch off the pathway, GTP needs to be hydrolysed to GDP [15]. While Ras has intrinsic GTPase activity, GTPase-activating proteins (GAPs) play a role in hydrolysing GTP to GDP by increasing GTPase activity by five orders of magnitude [16]. GAPs have an arginine finger and finger loop which probe into the Ras active site, stabilised by a secondary arginine residue, which bind Ras-GTP and promote GTP hydrolysis via stabilising the transition state and the switch regions of Ras [17].

1.1.2 PI3K/Akt pathway

The phosphoinositide 3-kinase (PI3K)/Akt pathway is another important signalling pathway with a role in cell survival, growth, proliferation, angiogenesis, metabolism and migration [18]. The PI3K/Akt pathway can be activated via one of three ways, all beginning with the binding of a GF to RTKs, causing dimerisation and autophosphorylation, as described for the MAPK/ERK pathway [19]. The activated RTKs can then interact with a protein containing a SH2 domain, such as directly to p85, the regulatory subunit of PI3K, which when phosphorylated relieves its inhibition on p110, the catalytic subunit of PI3K, or to Grb2 [20, 21]. Grb2 can then bind GAB, a docking protein, which binds p85 of PI3K, or it can recruit SOS which activates Ras [19]. Activated Ras can then activate p110, independent of p85, via relieving autoinhibition [22].

Activated PI3K then converts phosphatidylinositol 4,5-biphosphate (PIP2) to phosphatidylinositol 3,4,5-triphosphate (PIP3) at the plasma membrane [19]. PIP3 binds proteins with pleckstrin homology (PH) domains thus recruiting Akt and phosphoinositide-dependent kinase 1 (PDK1) to the plasma membrane, allowing PDK1 to partially activate Akt via phosphorylate T308 [23, 24]. Full activation of Akt occurs upon the phosphorylation of S473 [23]. Once activated, Akt can phosphorylate downstream signalling proteins, which either inhibits them, in the case of GSK3, or activates them, in the case of MDM2, both of which lead to cell proliferation and survival [18].

Downstream signalling from Akt is stopped via dephosphorylation of PIP3 to PIP2 by phosphatase and tensing homolog (PTEN) or dephosphorylation of Akt at T308 by protein phosphatase 2 (PP2A) or at S473 by pleckstrin homology domain leucine-rich repeat protein phosphatase (PHLPP) [25].

1.1.3 Ras

There are three Ras proto-oncogenes within the GTPase family; HRas, KRas and NRas, with alternative splicing of KRas encoding KRas4A and KRas4B [26]. When mutated, most prevalently at residues G12, G13 and Q61, the 21 kDa Ras proteins have the potential to be tumour-causing due to uncontrolled cell proliferation [2, 27]. These mutations have been found in the early stages of tumour progression but have also shown to be important for tumour maintenance [28]. Mutations in Ras relates to multiple hallmarks of cancer, as outlined by Hanahan and Weinberg, including self-sufficiency in growth signals, evading apoptosis, limitless replicative potential and sustained angiogenesis [29]. In fact, Ras has shown to be mutated in 33% of all human cancers, with KRas being the most frequently mutated isoform [2]. Mutations in KRas are mainly found in pancreatic, colorectal and lung cancers, while HRas mutations are found in dermatological and head and neck cancers, and NRas mutations are common in melanomas and haematopoietic cancers [30]. These mutations impair GTP hydrolysis, leading to Ras persistently being bound to GTP and thus induce uncontrolled MAPK/ERK and PI3K/Akt pathway signalling [28]. Additionally, mutated Ras has shown to upregulate activation of wild type Ras via allosteric activation of the GEF SOS [31].

There have been many attempts to target Ras therapeutically, however, failures led to it becoming known as an undruggable target [28]. Direct inhibition attempts have produced compounds which are not potent enough or contain toxic functional groups, such as hydroxylamine [28]. Mutant-specific inhibitors show the promise of targeting cancer cells with mutated Ras, rather than inhibiting wild type Ras, however achieving selectivity for the different mutations, particularly mutated KRas, was a challenge [28]. The interactions between Ras and

other members of the pathway, such as Raf and SOS, have also been investigated for possible modulation, leading to the identification of low potency compounds and a peptide, which have the potential for optimisation [28]. The design of peptide mimics of the αH helix of SOS, which binds in the cleft of Ras containing switch 1 and switch 2 regions, demonstrated that inhibition of the Ras-SOS interaction is a possible therapeutic target [32].

More recently, break-through research has identified inhibitors of Ras. A KRas G12C specific compound has been identified and taken forward to clinical trials [33]. The AMG 510 compound binds in a surface groove and causes almost complete reduction in phosphorylated ERK after two hours of treatment, as well as showing specificity in inhibiting mutant tumours *in vivo* [33]. AMG 510 was designed from ARS-1620, which was a development from ARS-853, another KRas G12C specific inhibitor [33-35]. ARS-853 targets the switch 2 region of the inactive KRas protein, demonstrating high efficacy and low micromolar potency in cells [34]. ARS-853 has also demonstrated synergistic effects with potent and selective inhibitors of SOS1 [36]. These SOS1 inhibitors decrease phosphorylated ERK levels in cells by approximately 50% after 24 hours of treatment, due to KRas mutants being less dependent on SOS compared to wild type KRas [36]. There is a second isoform of SOS in humans, which could also be targeted therapeutically, therefore it is important to further elicit the roles of both the human SOS isoforms.

1.2 Son of Sevenless (SOS)

The first Ras GEF to be identified was the CDC25 gene product of *Saccharomyces cerevisiae*, a type of yeast, which was reported to promote exchange of GDP to GTP on Ras [37]. Following this discovery, other homologs with a highly conserved catalytic domain have been identified including in drosophila [38], mice [39] and rats [40]. The rat homolog was used as a probe to screen for human SOS, with an approximately 150 kDa protein being identified as SOS1 [40]. Human SOS2 was found to share a 69% amino acid identity [40].

Human SOS1 and SOS2 are multidomain protein with 1333 and 1332 residues, respectively [8]. Although they share some sequence identity, SOS1 and SOS2 are encoded on two separate chromosomes; SOS1 on 2p22 → p16 and SOS2 on 14q21 → q22 [41]. The domains in both isoforms, with the residue numbers of SOS1 given, include the histone domain (HD) (1-198), Dbl-homology (DH) domain (198-404), Pleckstrin-homology (PH) domain (404-550), Ras exchanger motif (Rem) (550-750), cdc25 domain (750-1050) and poly-proline (PxxP) domain (1050-1333), as illustrated in figure 2 [42].

Figure 2: Schematic of the SOS domains. Both SOS isoforms are made up of the histone domain (cyan), DH-PH unit (green), catalytic domain (magenta) and the poly-proline domain (red).

1.2.1 The role of the N-terminal of SOS

The N-terminal of SOS is made up of three domains: the Dbl-homology (DH) and Pleckstrin-homology (PH) domains, making up the DH-PH unit, and the histone domain, which link to the catalytic domain of SOS (figure 3). The coupling of the DH-PH unit and the histone domain allow for an increased efficiency of membrane binding by SOS, as well as activation of SOS via the release of autoinhibition [43].

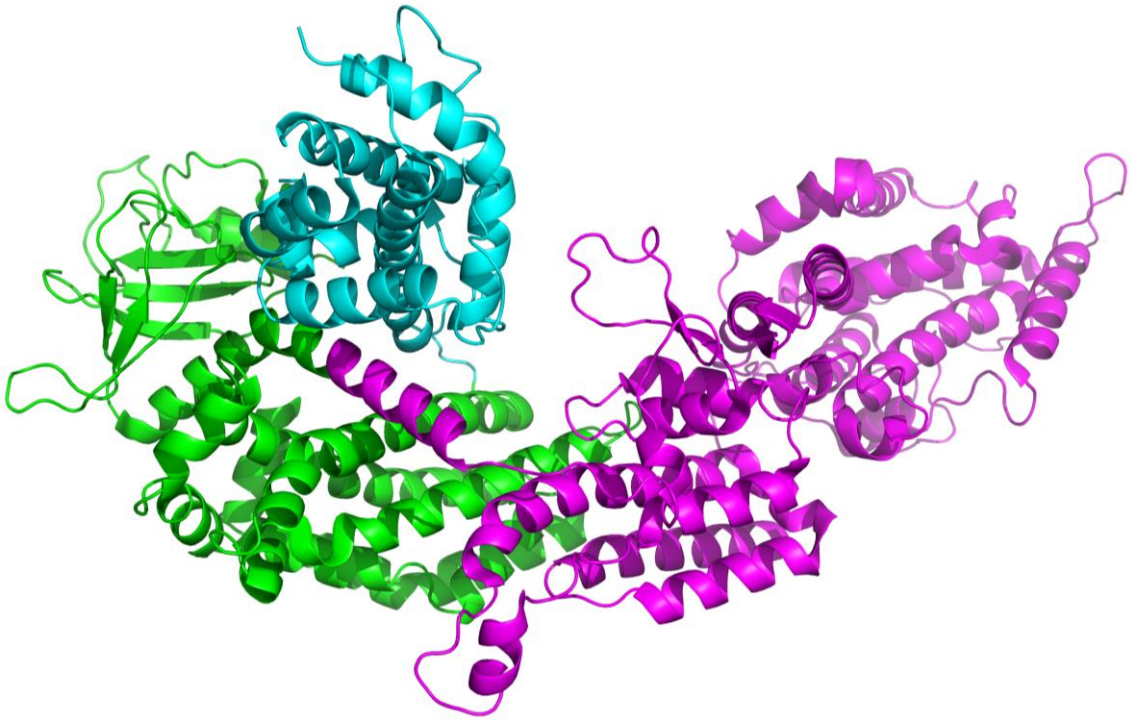

Figure 3: Structure of the N-terminal and catalytic domain of SOS1. The structure includes the histone domain (cyan), DH-PH unit (green) and catalytic domain (magenta) of SOS1. Structure generated using PyMOL with PDB file 3KSY [43].

The PH domain in the DH-PH unit plays a role in membrane localisation via binding to phospholipids, including PIP2 and phosphatic acid (PA) [44]. The PH domain can localise SOS to the plasma membrane without the SH3 domain of Grb2 binding the poly-proline domain of SOS [45]. This additional tether of the PH domain of SOS to the plasma membrane in the presence of the PIP2 and PA phospholipids increases SOS activation [46]. This is due to an increased concentration of SOS at the plasma membrane which helps Ras-GTP overcome the N-terminal inhibition and insert into the allosteric site of SOS [46]. This N-terminal inhibition is caused by the DH domain in the DH-PH unit positioning in such a way to block the allosteric Ras binding site, thus autoinhibiting SOS activation [47]. Additionally, this block reduces the affinity of the SOS catalytic domain for Ras [47].

The DH domain of SOS is also a GEF for Rac, a member of the Rho family who activates JNK, but not other family members such as RhoA [48]. However, in the presence of the PH domain, this activity is inhibited, shown by a failure to activate JNK, indicating the role of the PH domain in the regulation of the activity of the DH domain [48]. This inhibition is reversed when the DH-PH unit is co-expressed with Ras, potentially via the PI3K pathway which phosphorylates PIP2 to PIP3 on the plasma membrane, a phospholipid that the PH domain can bind [48].

The histone domain contains two histone folds which closely resembles two core nucleosomal histones, H2A and H2B [42]. They interact mainly via their hydrophobic residues to form a pseudodimer structure similar to histone fold dimers [42]. This pseudodimer binds the rest of the SOS protein by a tight interaction of two aspartic acid residues with an arginine residue in the helical linker between the PH and Rem domains [49]. Mutations of the arginine residue are found in Noonan syndrome, where they cause enhanced activation of Ras and ERK, indicating an autoinhibitory role of the N-terminal of SOS [50, 51]. Specifically, the histone domain plays two roles; assisting with blocking of the allosteric site of SOS and stabilising the DH-PH unit in an inhibitory conformation [43]. The histone domain stabilises the inhibitory conformation by anchoring the PH-Rem linker and fixing the position of the DH domain [43].

When in the autoinhibitory conformation, the histone domain orientates with a negative charge towards the negatively charged membrane [43]. A conformational change is required to expose the positively charged surface of the histone domain to the plasma membrane, which would allow the histone domain to bind PA lipids [52]. The binding of the histone domain to PA lipids increases membrane localisation of SOS due to providing an additional membrane anchoring point, as well as increasing SOS activation through the histone domain-PA interaction in an unknown mechanism [52]. Additionally, this conformational change disrupts the interaction between the histone domain and the Rem-PH helical linker, destabilising the autoinhibitory

conformation of the DH-PH unit, thus allowing SOS activation through the binding of Ras-GTP to the allosteric site of SOS [52].

1.2.2 The role of the catalytic site of SOS

The catalytic site of SOS is made up of the Ras exchanger motif (Rem) domain and the cdc25 domain, named after its homology to the cdc25 protein in *Saccharomyces cerevisiae* [42]. These domains have been found to bind two Ras molecules per SOS molecule, one in the active site and the other in the allosteric site (figure 4).

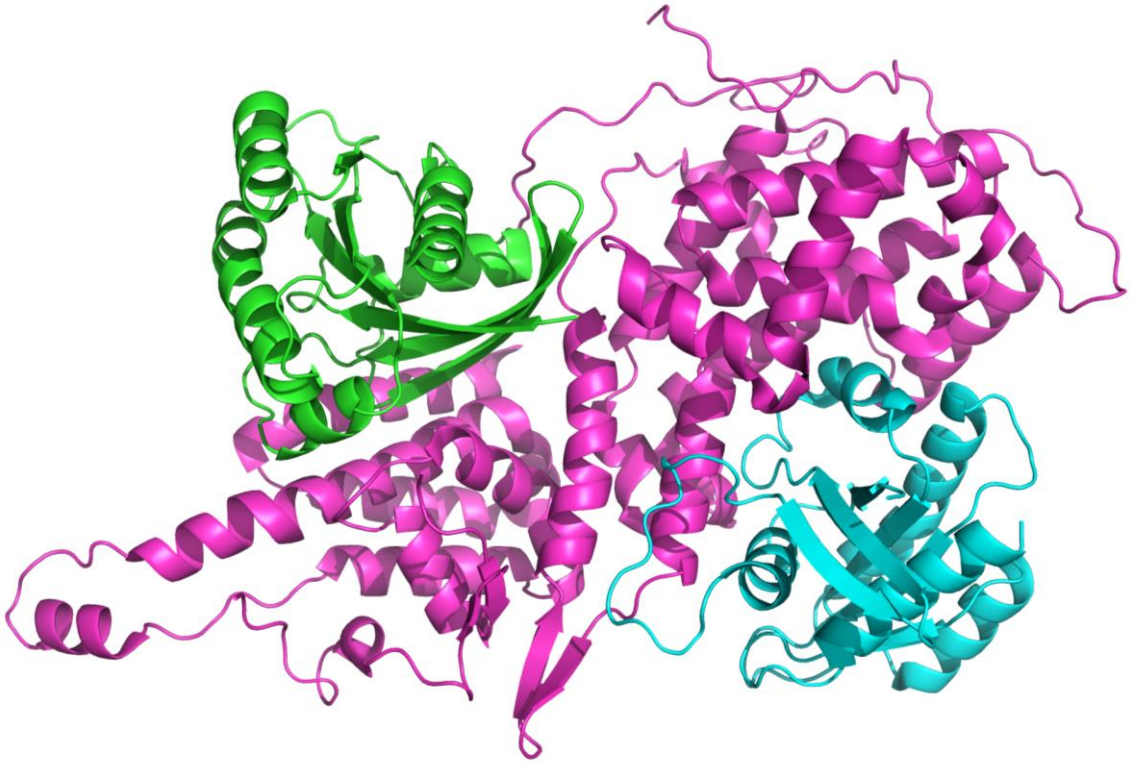

Figure 4: Two molecules of Ras can bind SOS simultaneously. The structure shows the catalytic domain of SOS1 (magenta) bound to two Ras molecules, one in the active site (green) and another in the allosteric site (cyan). Structure generated using PyMOL with PDB file 1NVW [53].

The cdc25 domain of SOS binds Ras-GDP in the active site and induces conformational changes in the switch 1 and switch 2 regions of Ras. A helical hairpin of SOS displaces the switch 1 region of Ras, blocking magnesium and phosphate of the nucleotide binding [54]. Switch 2 is held by SOS, restructuring the backbone of Ras to exclude the nucleotide by preventing the coordination of the magnesium and phosphate [54].

Ras-GTP binds to the SOS allosteric site in the Rem domain and cdc25 domain via its switch 1 and switch 2 regions [53]. When in the GDP bound state, Ras residues in the switch 1 and switch 2 regions bind 10 times weaker to the allosteric site of SOS compared to the GTP bound state, due to a conformational change offered by GTP loading to allow for tight binding of Ras to the allosteric site on SOS [47, 53]. Binding of Ras-GTP causes a rotation of the Rem domain of SOS by about 10 degrees [53]. While this rotation has little effect on the conformation of the active site of SOS, it allows hydrogen bonds to form between switch 1 of Ras in the active site and the Rem domain as well as a helical hairpin [53]. The presence of Ras-GTP in the allosteric site also showed increased release of GDP from Ras catalysed by SOS, indicating a positive feedback loop [53].

1.2.3 The role of the C-terminal poly-proline domain of SOS

The C-terminal of the SOS contains a proline-rich domain. Both SH3 domains in Grb2, located at its N-terminal and C-terminal regions, bind SOS via this poly-proline region in two distinct locations [55]. This binding allows Grb2 to localise SOS to the RTK via Grb2 binding to phosphorylated tyrosine residues on the RTK through its SH2 domain [6]. SOS can also bind tyrosine kinase substrates such as the Shc protein, however requires Grb2 to form this complex [55]. Upon phosphorylation of SOS, the Grb2-SOS complex dissociates, removing a tether of SOS to the plasma membrane [56].

Additionally, the poly-proline domain has been shown to obstruct Ras binding to the allosteric binding site of the catalytic domain [57]. However, the structure of SOS including the poly-proline domain remains to be solved, likely due to its intrinsically disordered nature [58]. This autoinhibition occurs independently of N-terminal inhibition, yet both mechanisms were shown to be required for complete inhibition of SOS binding with Ras [57].

1.2.4 The differences between the two human isoforms of SOS

The SOS1 and SOS2 proteins are both ubiquitously expressed [59]. Although the abundance of proteins in the MAPK/ERK pathway varies between cells, SOS1 and SOS2 are both found at low levels in all cell types compared to that of other core proteins and some regulatory proteins [60]. SOS1 has a slightly higher abundance than SOS2, as well as having a longer half-life, with the instability of SOS2 linked to ubiquitin degradation [60, 61].

The two isoforms show a difference in their binding to activated RTKs via Grb2, with SOS1 showing preferential binding over SOS2 [62]. The presence of SOS1, with SOS2, increases long-term ERK activation following stimulation of the RTK EGFR, compared to without SOS1 [62]. SOS forms a complex with activated EGFR via Grb2, with the SOS1 complex binding short- and

long-term, while SOS2 only binds short-term [62]. Interestingly, SOS2 has a higher binding affinity for Grb2, *in vivo* and *in vitro*, despite both proteins binding via both of SH3 domains in Grb2 [63]. Significant differences between the sequences in the C-terminal of SOS1 and SOS2 have been identified. Specifically, residues 1126 to 1242 in SOS2 contain three perfectly matched XPpXP motifs, while the equivalent region in SOS1 contains only one, leading to a higher affinity of SOS2 for Grb2 potentially due to an increased number of high affinity binding sites and/or the location of binding site for SOS2 [63]. Additionally, phosphorylation of SOS1, which leads to the dissociation of the SOS-Grb2 complex, is dependent on ERK, while that of SOS2 is mainly independent [64].

While SOS1 null mice were not embryonically viable, SOS2 null mice survived and developed normally, with no obvious defects [62, 65]. Interestingly, when inducible SOS1 null mice were engineered to study SOS1 and SOS2 knock-out in adult mice, the SOS isoforms demonstrated functional redundancy in full organism survival, while double knock-out mice were unable to survive past two weeks of SOS1 knock-out induction [66].

In mouse embryonic fibroblasts (MEFs), knock-out of SOS1 reduced proliferation compared to wild type and SOS2 knock-out MEFs, with double knock-out of SOS1 and SOS2 blocking cell proliferation [67]. SOS2 knock-out in MEFs expressing G12V mutant Ras isoforms and cells harbouring Ras mutations, demonstrated that SOS2 is not a critical mediator of proliferation [68, 69]. However, in the same cells, SOS2 was shown to be important for cellular transformation, with a decreasing hierarchy from mutant KRas to mutant HRas [68, 69]. Additionally, SOS2 requirement in MEFs was shown for other G12, G13 and Q61 KRas mutations, however, was least critical for MEFs expression Q61 mutated KRas [68].

In SOS2 knock-out MEFs expressing mutant Ras, activation of mutant Ras isoforms is not dependent on SOS2, shown by GTP loading of Ras [68]. However, single knock-out of both SOS1 and SOS2 decreased ERK phosphorylation, compared to wild type MEFs, while double-knock of SOS1 and SOS2 caused a significant decrease in phosphorylated ERK compared to wild type MEFs [67]. While knock-out of SOS2 did not significantly reduce ERK phosphorylation in MEFs harbouring mutated Ras, it did reduce Akt phosphorylation and blocked prolonged PI3K/Akt signalling [68]. This reduction was also observed in cells harbouring Ras mutations, except in a cell line known to phosphorylate Akt independent of wild type Ras [69]. The Ras isoform hierarchy for SOS2 in transformation is also mirrored for PI3K signalling, with constitutively activated PI3K able to promote KRas-driven transformation in MEFs with knock-out of SOS2 [68].

Overall, this implicates SOS1 as a vital protein, with SOS2 unable to compensate during development of mice or cell proliferation. However, it shows an importance of SOS2 in KRas

driven transformation and the PI3K/Akt pathway, as well as functional redundancy in adult mice. Additionally, knock-out of SOS2 was shown to reduce cell viability only in cells harbouring KRas mutations and not HRas or NRas mutations, indicating the therapeutic inhibition of SOS2 will most likely only prove effective in patients harbouring cancers with KRas mutations [69]. Encouragingly, SOS2 knock-out showed synergism with trametinib, a MEK inhibitor, to block proliferation and transformation of tumours cells harbouring KRas G12 mutations [68].

1.3 Artificial binding proteins

The majority of research into SOS has focussed on SOS1. However, if SOS is to be targeted therapeutically to modulate signalling in Ras-driven cancers, then the roles of both isoforms in the MAPK/ERK and PI3K/Akt signalling pathways need to be further elucidated. Artificial binding proteins could provide a novel approach to characterise the function of these proteins without the need for knocking down or overexpressing the whole protein. Artificial binding proteins are protein scaffolds with molecular recognition regions that can be generated in different ways, such as fusing a peptide with a known target to a scaffold with favourable characteristics, or via isolation from large protein libraries by display techniques [70]. Following generation, they can then be used therapeutically, diagnostically or in basic and applied research [71]. Ras has already been targeted by artificial binding proteins, specifically DARPins, monobodies and Affimer reagents.

1.3.1 Designed ankyrin repeat proteins (DARPin)

Designed ankyrin repeat proteins (DARPins) were designed based off the natural ankyrin repeat protein consisting of modules of a β-turn with 33 amino acid residues followed by two anti-parallel helices and a loop connecting to the next β-turn [72]. Repeats of two to four modules, containing seven randomised positions per module, and capping repeats at the N-terminal and C-terminal, allowed for a diverse library of DARPins to be obtained [72]. DARPins against Ras were screened for by phage display, giving rise to the Ras inhibitors DARPin K27 and K55 [73]. DARPin K27 inhibits nucleotide exchange by binding preferentially to Ras-GDP close to the switch regions, as shown in figure 5, while DARPin K55 inhibits the Ras-Raf interaction [73]. Additionally, DARPins specifically against KRas have been identified, namely K13 and K19, which bind to the allosteric lobe, inhibiting nucleotide exchange and KRas dimerisation [74]. This demonstrates the potential to obtain artificial binding proteins against a specific isoform of a target protein.

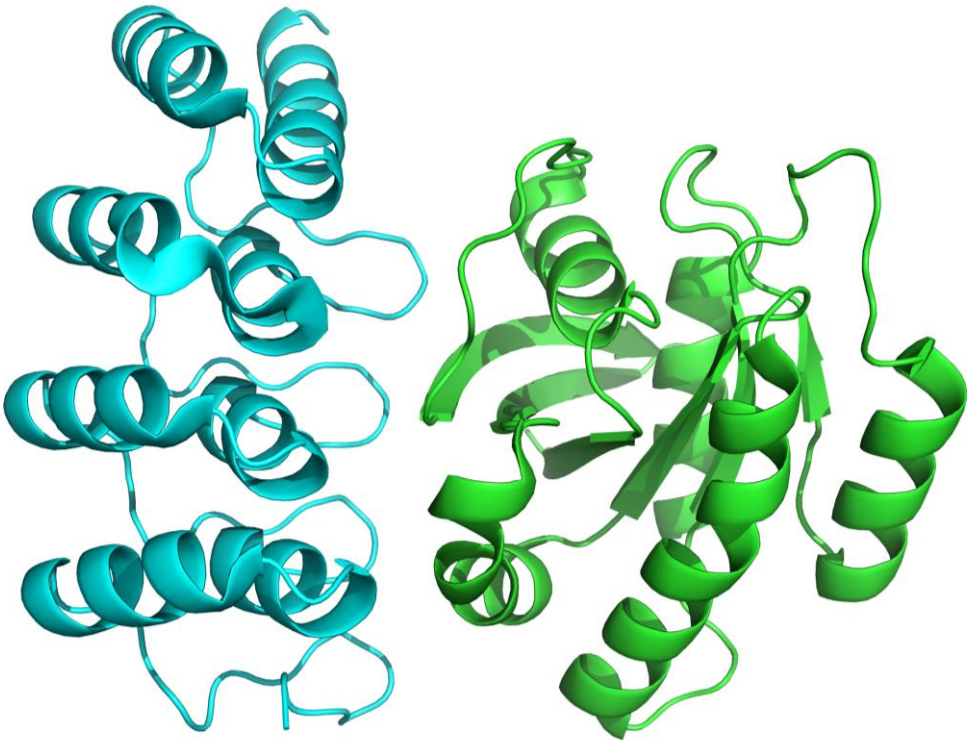

Figure 5: DARPin K27 binds to KRas. Structure of DARPin K27 (cyan) in complex with KRas (green). Structure generated using PyMOL with PDB file 5O2T [73].

1.3.2 Monobodies

Monobodies were designed using the tenth unit of fibronectin type III domain (FN3) [75]. They are small, monomeric proteins with a β-sandwich structure of seven β-strands [75]. The monobody NS1 was isolated as a specific inhibitor of KRas and HRas, not NRas, via a combinatorial library selection process [76]. Monobody NS1 has contacts with Arginine 135 in HRas, shown in figure 6, which is conserved in KRas but not NRas [76]. Like DARPins K13 and K19, monobody NS1 binds to the allosteric lobe of Ras, specifically HRas, opposite the switch 1 and switch 2 regions [76]. This lobe is also the location of the α4-α5 dimer interface in Ras, hence monobody NS1 binding disrupts Ras dimerisation and nanoclustering of KRas and HRas leading to decreased Raf activation [76]. Monobody NS1's ability to inhibit KRas has also been demonstrated *in vivo* using a chemically regulated version of monobody NS1 which inhibited signalling and proliferation of KRas-driven tumours [77]. This demonstrates the potential of using artificial binding proteins as pharmacophores to design effective therapeutics.

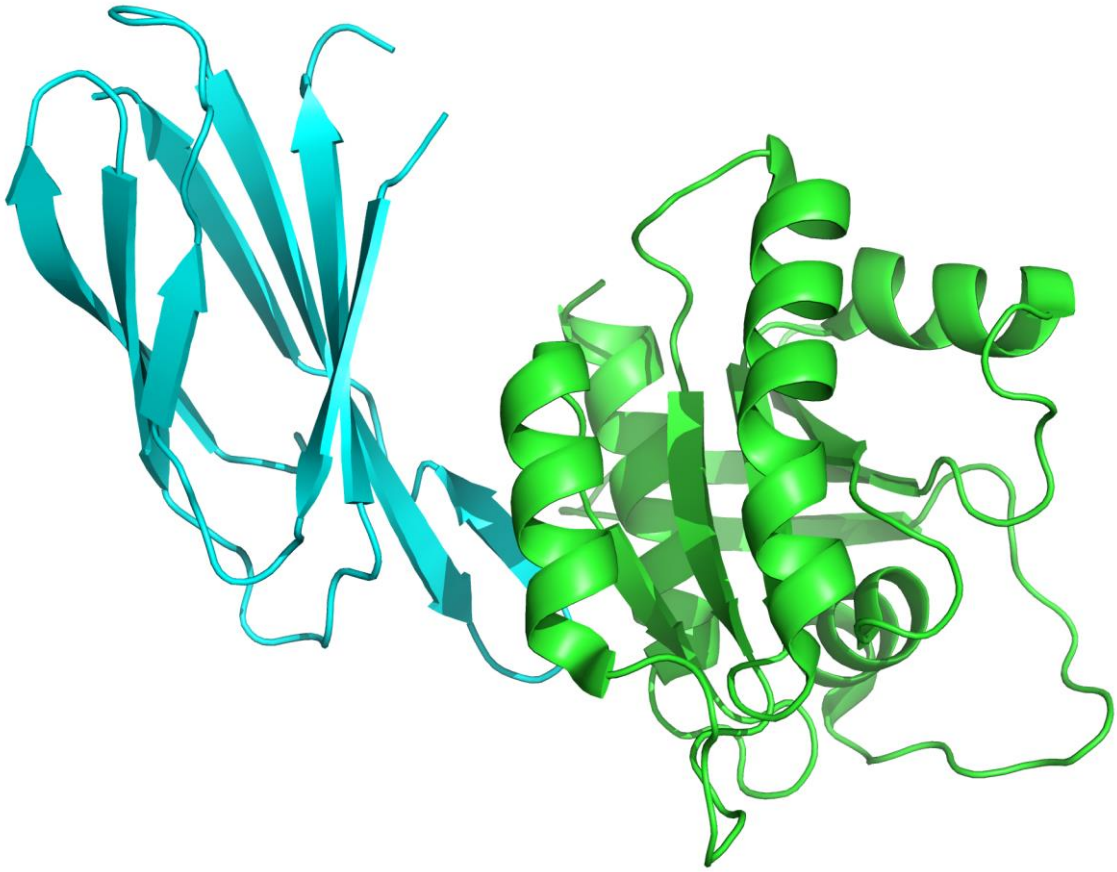

Figure 6: Monobody NS1 binds to HRas. Structure of Monobody NS1 (cyan) in complex with HRas (green). Structure generated using PyMOL with PDB file 5E95 [76].

1.3.3 Affimer reagents

The Affimer reagent scaffold types were derived from both a cystatin consensus sequence and the human Stefin A [78]. Both scaffolds contain two variable regions (VR) of nine amino acid residues, allowing Affimer reagents to bind to their target molecule in a similar manner to an antibody (figure 7) [79]. Benefits of Affimer reagents include their small size, as well as their stability in acidic environment and at high temperatures [78]. Affimer reagents have been reported to being used for modulation of protein function, detection of small molecules and cell imaging [78]. To obtain tightly binding Affimer reagents, Affimer phage libraries are screened against the target protein in a biotinylated form via phage display [79]. Additionally, negative selection can be used to deselect against an isoform during the second round of panning [80]. Following screening, positive binders are characterised via phage ELISA to determine binding specificity [79]. Phage ELISA may also contain the isoform which was deselected against, to confirm that positive binders are not cross-reactive. These Affimer reagents can then be further

characterised to determine their effects on the target protein, their site of binding and other traits.

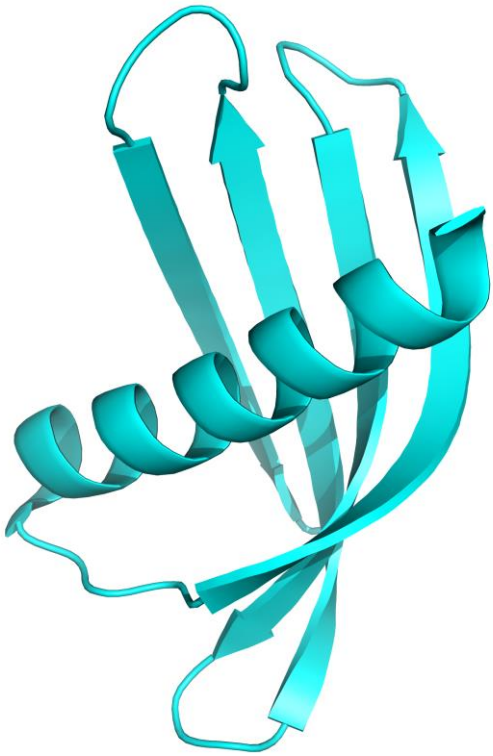

Figure 7: The Affimer scaffold. Structure of the Affimer scaffold where the VRs are located between two beta sheets. Structure generated using PyMOL with PDB file 4N6T [79].

The Tomlinson group have isolated Affimer reagents against KRas by phage display [81]. Affimer reagents shown to inhibit Ras function by a blocking nucleotide exchange were then used as pharmacophores to design compounds. Additionally, Affimer reagents against SOS1 have been isolated, with some SOS1 inhibitors also demonstrating SOS2 binding cross-reactivity. Therefore, the aim of this project is to isolate SOS2 binding Affimer reagents, both selective for SOS2 and cross-reactive between SOS1 and SOS2. These will then be tested for inhibitory properties, as inhibitors could be used to further elicit the role of SOS2 in Ras mediated cancer signalling.

2. Methods

2.1 Transformation of Plasmid DNA

XL-1 Blue Supercompetent *E. coli* cells (Agilent Technologies) were used for purification of plasmid DNA, while BL21 Star™ (DE3) chemically competent *E. coli* cells (Life Technologies) were used for protein expression. In-house stocks were generated using a rubidium chloride competent cell protocol.

Plasmid DNA (pET11a for Affimer reagents, KRas and $SOS2^{cat}$ or pET28c for $SOS1^{cat}$) was thawed and 70-100 ng in a 1 µL volume aliquoted into a pre-chilled 1.5 mL Eppendorf tube. The appropriate competent cells were thawed on ice and 10 µL of cells added to the pre-chilled plasmid DNA, the tube flicked to mix and incubated on ice for 30 minutes. Cells with plasmid DNA were heat shocked at 42°C in a water bath for 45 seconds. Heat shocked cells were incubated on ice for 2 minutes and then 190 µL LB broth (Invitrogen) was added. This was incubated at 37°C for 1 hour with shaking at 230 rpm. Following incubation, 100 µL of transformation mix was plated onto LB agar (Invitrogen) plates with the corresponding antibiotic (table 1) (termed LB-carb or LB-kana plates, collectively LB plates) and incubate overnight at 37°C.

	Affimer	**KRas**	**$SOS1^{cat}$**	**$SOS2^{cat}$**
Antibiotic type	Carbenicillin	Carbenicillin	Kanamycin	Carbenicillin
Concentration (µg/mL)	100	100	50	100

Table 1: Antibiotic type and concentration used for each plasmid DNA.

2.2 Purification of Plasmid DNA

Following transformation of plasmid DNA into XL-1 Blue *E. coli* cells (section 2.1), a single colony was picked from LB plates and placed in 5 mL LB broth with the corresponding antibiotic (table 1). This was incubated overnight at 37°C with shaking at 230 rpm.

Following overnight incubation, the culture was centrifuged at 4000 *x*g for 5 minutes. The supernatant was poured off and plasmid DNA extracted from cell pellets using a QIAprep Spin Miniprep kit (QIAGEN), following the manufacturer's instructions. DNA was eluted in 50 µL nuclease free water and absorbance at 260 nm (A_{260}) measured to determine DNA

concentration. Plasmid DNA was sent off to Genewiz for Sanger Sequencing using the T7 universal primer (5'-TAATACGACTCACTATAGGG-3').

2.3 Production and purification of His-tagged proteins

The individual conditions for protein production and purification are described in table 2.

		Protein			
		Affimer	**KRas**	**SOS1^{cat}**	**SOS2^{cat}**
Antibiotic	**Type**	Carbenicillin	Carbenicillin	Kanamycin	Carbenicillin
	Concentration (µg/mL)	100	100	50	100
Culture volumes	**Overnight culture volume (mL)**	2	5	5	5
	Culture volume (mL)	50	400	400	400
	Flask size (mL)	250	2,000	2,000	2,000
	Inoculation culture volume (mL)	1	5	5	5
Incubation conditions	**Temperature (°C)**	25	20	25	30
	Shaking speed (rpm)	150	180	150	150
	Time	Overnight	Overnight	Overnight	4 hours
Cell lysis	**Supplemented lysis buffer volume (mL)**	1	8	8	8
	Lysis tube	1.5 mL Eppendorf tube	15 mL falcon tube	15 mL falcon tube	15 mL falcon tube
	Lysis temperature	Room temperature	4°C	4°C	4°C
Incubation with Ni-NTA	**Centrifugation speed (*x*g)**	16,000	4,816 then 12,000	4,816 then 12,000	4,816 then 12,000
	Ni-NTA resin tube	1.5 mL Eppendorf tube	15 mL falcon tube	15 mL falcon tube	15 mL falcon tube
	Ni-NTA incubation temperature	Room temperature	4°C	4°C	4°C

Table 2: Protein production and purification conditions. The conditions used for Affimer, KRas, SOS1^{cat} and SOS2^{cat} proteins.

Following transformation of plasmid DNA into BL21 (DE3) *E. coli* cells (section 2.1), a single colony was picked from LB plates and placed in the overnight culture volume of LB broth with antibiotic and 1% glucose (table 2). This was incubated overnight at 37°C with shaking at 230 rpm.

Pre-warmed culture volumes of LB broth with antibiotic in flasks were inoculated with the overnight culture (table 2) and grown at 37°C with shaking at 230 rpm until an optical density of 600 nm (OD_{600}) of 0.6-0.8 was reached, or 0.8 for SOS2^{cat}. Cultures were then induced with

0.5 mM isopropyl β-d-1-thiogalactopyranoside (IPTG) and incubated with the relevant conditions (table 2).

Cells were harvested by centrifugation at 4,816 *x*g for 15 minutes. Once in 50 mL falcon tubes for 50 mL cultures or twice, first in beakers then in 50 mL falcon tubes, for 400 mL cultures. The supernatant was poured off and pellets were then stored at -20°C until extraction of expressed protein.

For extraction and purification, buffers were prepared (table 3).

	Lysis	**Wash**	**Elution**
Affimer	50 mM NaH_2PO_4, 300 mM NaCl, 30 mM Imidazole, 10% Glycerol, pH 7.4	50 mM NaH_2PO_4, 500 mM NaCl, 30 mM Imidazole, pH 7.4	50 mM NaH_2PO_4, 500 mM NaCl, 300 mM Imidazole, 10% Glycerol, pH 7.4
KRas	50 mM Tris-HCl, 300 mM NaCl, 30 mM Imidazole, 5% Glycerol, pH 7.5	50 mM Tris-HCl, 500 mM NaCl, 30 mM Imidazole, 5% Glycerol, pH 7.5	50 mM Tris-HCl, 500 mM NaCl, 300 mM Imidazole, 5% Glycerol, pH 7.5
SOS	20 mM Tris-HCl, 300 mM NaCl, 30 mM Imidazole, 5% Glycerol, pH 8	20 mM Tris-HCl, 500 mM NaCl, 30 mM Imidazole, 5% Glycerol, pH 8	20 mM Tris-HCl, 500 mM NaCl, 300 mM Imidazole, 5% Glycerol, pH 8

Table 3: Protein extraction and purification buffers. Buffers used for extraction and purification of Affimer, KRas, $SOS1^{cat}$ and $SOS2^{cat}$ proteins. The same buffers were used for both $SOS1^{cat}$ and $SOS2^{cat}$ proteins.

The cell pellet was thawed and resuspended in lysis buffer (table 3) supplemented with 0.1 mg/mL lysozyme (Sigma-Aldrich), 1% Triton™ X-100 (Sigma-Aldrich), 10 U/mL Benzonase® Nuclease (Novagen®) and 1X Halt™ protease inhibitor cocktail (Thermo Scientific) (table 2). Cell-lysis buffer mixture was transferred to the relevant tube and incubated for 1 hour at the relevant temperature on a rotator (table 2). Affimer protein was then heat denatured by incubation at 50°C for 20 minutes.

Cell debris was pelleted by centrifugation for 20 minutes at 4 °C, once for 50 mL cultures or twice for 400 mL cultures (table 2). Meanwhile, 300 µL Amintra Ni-NTA slurry (Expedeon) was washed three times in lysis buffer (table 3) to obtain 150 µL resin. The supernatant, containing the soluble fraction, was transferred to the tube containing the Ni-NTA resin and incubated for 1-2 hours at the relevant temperature on a rotator (table 2). A 10 µL sample of the soluble fraction was taken and frozen for analysis by SDS-PAGE.

Following incubation, Pierce™ 2mL disposable columns (ThermoFischer) were equilibrated by applying 3 mL wash buffer (table 3) and allowing it to empty by gravity. The resin-soluble protein

mix was then transferred to the column, allowing it to empty by gravity. A 10 µL sample of the unbound fraction was taken. The resin was then resuspended in 3 mL wash buffer (table 3), allowing to empty by gravity. 10 µL samples of the first and the last wash were taken, with the last wash being determined by an absorbance at 280 nm (A_{280}) reading of < 0.09. His-tagged protein was eluted by resealing the column and resuspending the resin in 0.5 mL for Affimer or 0.3 mL for KRas and SOS elution buffer (table 3) and incubated for 5 minutes, before removing the cap and allowing to empty via gravity. This was repeated until no more protein was eluted, by measurement of A_{280} < 0.5. Elutions were collected and 10 µL samples from each taken. Affimer and KRas elutions were snap frozen and stored at -80°C, while SOS elutions were dialysed immediately (section 2.5).

All collected fractions were mixed with sample buffer (2% SDS, 50 mM Tris pH 7, 5% glycerol, bromophenol blue) containing β-mercaptoethanol, boiled for 5 minutes at 95°C, and run on a 15% SDS-PAGE with PageRuler Pre-stained Protein ladder, 10 to 180 kDa (Thermo Scientific), for 1 hour at 150 V until sample buffer visibly ran to the bottom of the SDS-PAGE. SDS-PAGE was stained with Coomassie blue for 1 hour and destained overnight. Destained SDS-PAGE was imaged colourimetrically using the Amersham Imager (GE Life sciences).

2.4 Protein expression trials of SOS2^{cat}

Following transformation of SOS2^{cat} plasmid DNA into BL21 (DE3) *E. coli* cells (section 2.1), a single colony was picked from the LB plate and placed in 5 mL LB broth containing 100 µg/mL carbenicillin and 1% glucose. Four 250 mL flasks with 50 mL LB containing 100 µg/mL carbenicillin were inoculated with 1 mL overnight culture and incubated at 37°C, 230 rpm until two flasks reached an OD_{600} of ~0.6 and the other two flasks reached OD_{600} ~0.8. Samples of 1 mL from each flask were taken, spun down and the pellets was frozen. Flasks were then induced with 0.5 mM IPTG. One flask from each OD_{600} was then incubated at 25°C with shaking at 150 rpm and the other at 30°C with shaking at 150 rpm. A 1 mL sample was taken from each flask at 4 hours, 6 hours and following overnight incubation. These samples were spun down and the pellets frozen.

The cell pellets were thawed and resuspended in 50 µL SOS lysis buffer (table 3) supplemented with 0.1 mg/mL lysozyme, 1% Triton™ X-100, 10 U/mL Benzonase® Nuclease and 1X Halt™ protease inhibitor cocktail. Cell-lysis buffer mixtures were incubated for 20 minutes at 4°C on a rotator. Cell debris was pelleted by centrifugation for 20 minutes at 16000 *x*g at 4 °C. The supernatant containing the soluble fraction was taken and mixed with sample buffer containing β-mercaptoethanol, boiled for 5 minutes at 95°C, and run on a 15% SDS-PAGE with PageRuler Pre-stained Protein ladder, 10 to 180 kDa, for 1 hour at 150 V until sample buffer visibly ran to

the bottom of the gel. SDS-PAGE was stained with Coomassie blue for 1 hour and destained overnight. Destained SDS-PAGE was imaged colourimetrically using Amersham Imager.

2.5 Dialysis of SOS1^{cat} and SOS2^{cat}

Purified SOS1^{cat} or SOS2^{cat} protein were aliquoted into Pur-A-Lyzer™ mini dialysis tubes (Sigma-Aldrich) and dialysed in buffer containing 50 mM Tris-HCl, 100 mM NaCl and 1 mM DTT, pH 7.5. SOS elutions were dialysed at 4°C with stirring and buffer changes after the first hour and again after overnight for the last hour. SOS was then spun down at 10,000 *x*g for 10 minutes to pellet any precipitate. Aliquots of 200 µL were snap frozen and stored at -80°C. The concentration was determined by Pierce™ BCA protein assay kit (Thermo Scientific), following the manufacturer's instructions.

2.6 Nucleotide loading of KRas with mGDP (KRasmGDP)

Per 130 µL purified KRas, two 0.5 mL Zeba™ Spin Desalting columns, 7K MWCO (Thermo Scientific) were prepared with nucleotide loading buffer (20 mM Tris-HCl, 50 mM NaCl, 0.5 mM $MgCl_2$, pH 7.5), following the manufacturer's instructions. KRas was then buffer exchanged through one column and then the other. The A_{280} was measured and protein concentration determined using the extinction co-efficient of KRas. 30 µM KRas was combined with 60 µM Mant-GDP (mGDP; Invitrogen), 5 mM EDTA and 1 mM DTT in nucleotide loading buffer to a final volume of 124 µL. This was incubated for 1 hour on ice, protected from light. $MgCl_2$ to a final concentration of 45 mM was added, mixed and incubated for 30 minutes on ice, protected from light. Two more Zeba™ Spin Desalting columns were prepared per 130 µL mixture, this time with nucleotide exchange buffer (20 mM HEPES, 150 mM NaCl, 10 mM $MgCl_2$, pH 7.5), following the manufacturer's instructions. KRasmGDP was then buffer exchanged through the two columns. 20 µL aliquots of KRasmGDP were snap frozen and stored at -80°C. The concentration was determined by Pierce™ BCA protein assay kit, following the manufacturer's instructions.

2.7 SOS catalysed nucleotide exchange assays

Nucleotide exchange buffer was supplemented with 0.5 µM SOS1^{cat} or 1 µM SOS2^{cat}, and 0.4 mM GTP to make NES buffer. Samples, as described below (sections 2.7.1-6), were aliquoted into even wells of 384-well flat-bottomed, non-binding Corning plates in black with 25 µL per well, alongside SOS control (NES buffer), KRasmGDP control (nucleotide exchange buffer) and KRasmGDP-GTP control (nucleotide exchange buffer with 0.4 mM GTP). All in triplicate.

Nucleotide exchange buffer was supplemented with 1 µM KRasmGDP and 2 mM DTT and aliquoted with 20 µL per odd well, alongside the background control (40 µL nucleotide exchange

buffer). All in triplicate. The plate was covered and incubated for 10 minutes at 37°C. Following incubation, 20 µL from the even wells was pipetted into 20 µL KRasmGDP/DTT in the odd wells, quickly.

The plate was read every minute for 90 minutes with fluorescence measured at 440 nm after excitation at 365 nm on the Tecan Spark with the Mant-GDP assay protocol, with gains set to the KRas control well. Data was normalised and analysed using OriginPro software to determine the initial rates of nucleotide exchange.

2.7.1 Dialysis of Affimer proteins

Prior to use, Affimer proteins were aliquoted into Pur-A-Lyzer™ mini dialysis tubes and dialysed in buffer containing 20 mM HEPES, 150 mM NaCl, pH 7.5. Affimer proteins were dialysed for 2 hours at room temperature with stirring and then overnight at 4°C with stirring in fresh buffer. Dialysed proteins were spun down at 16,000 *x*g for 15 minutes to pellet any precipitant. The A_{280} of dialysed Affimer proteins was measured three times and the average concentration determined using the extinction co-efficient.

2.7.2 SOS1^{cat} catalysed nucleotide exchange assay with Affimer inhibitors for IC_{50} curves

Affimer proteins were dialysed as described in section 2.7.1. Affimer proteins were diluted to 20 µM in SOS1^{cat} NES buffer, with any lost SOS1^{cat} or GTP replaced. Serial dilutions were performed to make final concentrations of 10, 5, 2.5, 1.25, 0.63, 0.31, 0.16, 0.078, 0.039, 0.019 and 0.009 µM following mix with KRasmGDP/DTT. These samples were run alongside SOS1^{cat}, KRasmGDP, KRasmGDP-GTP and background controls.

2.7.3 SOS1^{cat} catalysed nucleotide exchange assay with individual Affimer inhibitors for alanine scanning

Affimer proteins were dialysed as described in section 2.7.1. Affimer proteins were diluted to 10 µM in SOS1^{cat} NES buffer, with any lost SOS1^{cat} or GTP replaced, for a final 5 µM concentration when mixed with KRasmGDP/DTT. These samples were run alongside SOS1^{cat}, KRasmGDP, KRasmGDP-GTP and background controls.

2.7.4 Optimisation of SOS2^{cat} catalysed nucleotide exchange assay

SOS2^{cat} was diluted to 2, 1.5, 1, 0.75, 0.5 and 0.25 µM in nucleotide exchange buffer supplemented with 0.4 mM GTP to give final concentrations of 1, 0.75, 0.5, 0.375, 0.25 and

0.125 µM following mix with KRasmGDP/DTT. These samples were run alongside SOS1^{cat}, KRasmGDP, KRasmGDP-GTP and background controls.

2.7.5 SOS2^{cat} catalysed nucleotide exchange assay with Affimer s18

Affimer proteins were dialysed as described in section 2.7.1. Affimer proteins were diluted to 20 µM in SOS2^{cat} NES buffer, with any lost SOS2^{cat} or GTP replaced, for a final 10 µM concentration when mixed with KRasmGDP/DTT. These samples were run alongside SOS2^{cat}, KRasmGDP, KRasmGDP-GTP and background controls.

2.7.6 SOS1^{cat} or SOS2^{cat} catalysed nucleotide exchange assay with JM83 expressed Affimer proteins

Affimer proteins were dialysed as described in section 2.13. Dialysed Affimer proteins at 12 µM were diluted to 10 µM in NES, either with 0.5 µM SOS1^{cat} or 0.5 µM SOS2^{cat}. SOS2^{cat} concentration was halved to keep Affimer to SOS ratio constant. These samples were run alongside SOS1^{cat} or SOS2^{cat}, KRasmGDP, KRasmGDP-GTP and background controls.

2.8 Site-directed mutagenesis of Affimer s18 alanine mutants

QuikChange® II Primers were designed to mutate each residue in the VRs of Affimer s18 to the alanine codon GCT individually using Agilent's QuikChange® Primer Design Program (https://www.agilent.com/store/primerDesignProgram.jsp) (table 4). Primers were produced by Sigma-Aldrich.

Primer name	Primer sequence (5' to 3')
1.1 F	TAAAGCGAAAGAACAGGCTTCTGAACGTTGGCCGC
1.1 R	GCGGCCAACGTTCAGAAGCCTGTTCTTTCGCTTTA
1.2 F	GCGAAAGAACAGACTGCTGAACGTTGGCCGCAT
1.2 R	ATGCGGCCAACGTTCAGCAGTCTGTTCTTTCGC
1.3 F	GTTAAAGCGAAAGAACAGACTTCTGCTCGTTGGCCGCATT
1.3 R	AATGCGGCCAACGAGCAGAAGTCTGTTCTTTCGCTTTAAC
1.4 F	TAAAGCGAAAGAACAGACTTCTGAAGCTTGGCCGCATTTCG
1.4 R	CGAAATGCGGCCAAGCTTCAGAAGTCTGTTCTTTCGCTTTA
1.5 F	GCGAAAGAACAGACTTCTGAACGTGCTCCGCATTTCGACACC
1.5 R	GGTGTCGAAATGCGGAGCACGTTCAGAAGTCTGTTCTTTCGC
1.6 F	CAGACTTCTGAACGTTGGGCTCATTTCGACACCATGTAC
1.6 R	GTACATGGTGTCGAAATGAGCCCAACGTTCAGAAGTCTG
1.7 F	ACTTCTGAACGTTGGCCGGCTTTCGACACCATGTACTAC
1.7 R	GTAGTACATGGTGTCGAAAGCCGGCCAACGTTCAGAAGT
1.8 F	ACTTCTGAACGTTGGCCGCATGCTGACACCATGTACTACCTGAC
1.8 R	GTCAGGTAGTACATGGTGTCAGCATGCGGCCAACGTTCAGAAGT

Primer name	Primer sequence (5' to 3')
1.9 F	GAACGTTGGCCGCATTTCGCTACCATGTACTACCTGACC
1.9 R	GGTCAGGTAGTACATGGTAGCGAAATGCGGCCAACGTTC
2.1 F	CTGTACGAAGCGAAAGTTTGGGTTAAGGCTGATAGATATCCAAGTTATATTTGGAAC
2.1 R	GTTCCAAATATAACTTGGATATCTATCAGCCTTAACCCAAACTTTCGCTTCGTACAG
2.2 F	GCGAAAGTTTGGGTTAAGCAGGCTAGATATCCAAGTTATATTTGG
2.2 R	CCAAATATAACTTGGATATCTAGCCTGCTTAACCCAAACTTTCGC
2.3 F	GAAGCGAAAGTTTGGGTTAAGCAGGATGCTTATCCAAGTTATATTTGGAACTTCAAA
2.3 R	TTTGAAGTTCCAAATATAACTTGGATAAGCATCCTGCTTAACCCAAACTTTCGCTTC
2.4 F	GAAGCGAAAGTTTGGGTTAAGCAGGATAGAGCTCCAAGTTATATTTGGAAC
2.4 R	GTTCCAAATATAACTTGGAGCTCTATCCTGCTTAACCCAAACTTTCGCTTC
2.5 F	CGAAAGTTTGGGTTAAGCAGGATAGATATGCTAGTTATATTTGGAACTTCAA
2.5 R	TTGAAGTTCCAAATATAACTAGCATATCTATCCTGCTTAACCCAAACTTTCG
2.6 F	TGGGTTAAGCAGGATAGATATCCAGCTTATATTTGGAACTTCAAAGAACTG
2.6 R	CAGTTCTTTGAAGTTCCAAATATAAGCTGGATATCTATCCTGCTTAACCCA
2.7 F	GTTAAGCAGGATAGATATCCAAGTGCTATTTGGAACTTCAAAGAACTGCAG
2.7 R	CTGCAGTTCTTTGAAGTTCCAAATAGCACTTGGATATCTATCCTGCTTAAC
2.8 F	TTGGGTTAAGCAGGATAGATATCCAAGTTATGCTTGGAACTTCAAAGAACT
2.8 R	AGTTCTTTGAAGTTCCAAGCATAACTTGGATATCTATCCTGCTTAACCCAA
2.9 F	GTTTGGGTTAAGCAGGATAGATATCCAAGTTATATTGCTAACTTCAAAGAACTGCAGG
2.9 R	CCTGCAGTTCTTTGAAGTTAGCAATATAACTTGGATATCTATCCTGCTTAACCCAAAC

Table 4: Primer sequences for Affimer s18 alanine scanning. Primer name denoting the mutated residue position and whether forward (F) or reverse (R) primer.

These primers were used for site-directed mutagenesis with KOD Hot Start DNA polymerase kit (Novagen®). Reactions were set up with Affimer s18 pET11a plasmid DNA following the manufacturer's instructions and run overnight with the programme outlined in table 5.

Name	Temperature (°C)	Time	
Initial denaturation	98	2 minutes	
Denaturation	98	20 seconds	20 cycles
Annealing	72	10 seconds	
Extension	70	3 minutes 30 seconds	
Final extension	70	5 minutes	
Store	4	Infinite	

Table 5: PCR programme standard protocol run for site-directed mutagenesis.

Methylated template DNA was digested with 0.5 µL *DpnI* (New England BioLabs; NEB) and incubated at 37°C for 1 hour. *DpnI* digested products were mixed with orange G loading dye and run on 1% agarose gel containing SYBR Safe DNA gel stain at 100 V for 30 minutes with Quick-Load purple 2-log DNA ladder (NEB). Agarose gel was imaged colourimetrically using the Amersham Imager.

Products producing a visible band in 1% agarose gel were cleaned up using FastGene® Gel/PCR extraction kit (Nippon Genetics), following the manufacturer's instructions. DNA was eluted with 30 µL nuclease free water and the A_{260} measured to determine DNA concentration. Plasmid DNA was then sent off to Genewiz for Sanger Sequencing using the T7 universal primer.

Products without visible band were repeated using a heat gradient PCR programme to troubleshoot. The protocol remained the same with only a difference in annealing temperatures by doing a gradient of 60, 63, 66, 70 and 72°C.

2.9 Biotinylation and characterisation of SOS1^{cat} and SOS2^{cat} (SOS1-B and SOS2-B)

EZ-link NHS biotin

SOS1^{cat} and SOS2^{cat} proteins were biotinylated via the sidechain of lysine residues using EZ-Link™ NHS Biotin (Thermo Scientific). Protein was incubated with NHS biotin at a 10-fold molar excess, diluted in DMSO, in a total volume of 100 µL PBS (phosphate-buffered saline) for 30 minutes at room temperature. Following incubation, the biotinylated proteins were run through Zeba™ Spin Desalting columns, equilibrated with PBS, to remove excess biotin. Aliquots were taken immediately for ELISA and BCA (Pierce™ BCA protein assay kit), while the rest was snap frozen and stored at -80°C for western blot analysis, the nucleotide exchange assay and phage display.

EZ-link HPDP biotin

SOS1^{cat} and SOS2^{cat} proteins were biotinylated via the sidechain of cysteine residues using EZ-Link™ HPDP Biotin (Thermo Scientific). Half the SOS2^{cat} sample was incubated with a double volume of PBS containing 1mM EDTA washed Pierce™ Immobilized TCEP Disulfide Reducing Gel (Thermo Scientific) for 1 hour at room temperature prior to biotinylation to reduce any disulfide bonds. Following incubation in TCEP resin or without, protein was incubated with a final concentration of 0.4 mM HPDP biotin for 2 hours at room temperature. Following incubation, the biotinylated proteins were run through Zeba™ Spin Desalting columns, equilibrated with PBS, to remove excess biotin. Aliquots were taken immediately for ELISA and BCA (Pierce ™ BCA protein assay kit), while the rest was snap frozen and stored at -80°C for western blot analysis, the nucleotide exchange assay and phage display.

ELISA

Varying concentrations of biotinylated protein were tested using an ELISA to check biotinylation. 50 µL PBS per well was aliquoted to a Nunc-Immuno™ MaxiSorp™ strips (Thermo Scientific) and then 1 µL, 0.1 µL, 0.01 µL and 0 µL biotinylated SOS protein was added. This was left to incubate overnight at 4°C. The following day, the strip was washed three times with PBST (PBS with 0.1% Tween-20) and then 250 µL 10X casein blocking buffer (Sigma) was aliquoted into each well and incubated at 37°C for 3 hours. Following incubation, the wells were washed again with PBST and 50 µL of Pierce™ High Sensitivity Streptavidin-HRP, diluted 1:1000 in 2X blocking buffer, was aliquoted into each well. This was incubated for 1 hour at room temperature on a shaker. Following incubation, the wells were washed 6 times with PBST and 50 µL SeramunBlau® fast TMB/substrate solution (Seramun Diagnostica) was aliquoted into each well. Wells were allowed to develop on shaker, following which absorbance at 620 nm (A_{620}) was measured and photographs taken.

Western blot analysis

Biotinylated protein samples were analysed via Western blot to validate ELISA results. NHS biotin samples were diluted to 0.1 mg/mL in 9 µL and mixed with 3 µL sample buffer containing β-mercaptoethanol, while HPDP biotin samples were diluted to 0.4 mg/mL in 2 µL and mixed with 7 µL water and 3 µL sample buffer without β-mercaptoethanol, to prevent reduction of the disulfide bond between SOS and biotin. Samples were boiled for 5 minutes at 95°C. Samples were run with 10 µL per well on 15% SDS-PAGE gel at 150V for 1 hour. Protein was transferred to a nitrocellulose membrane using the Trans-Blot Turbo Transfer system (Bio-Rad). The membrane was blocked with 5% w/v milk-TBST (tris-buffered saline with 0.2% Tween-20) overnight at 4°C. The membrane was probed with Pierce™ High Sensitivity Streptavidin-HRP diluted to 1:10,000 in 5% w/v milk-TBST for 1 hour at room temperature. The membrane was washed with three short washes followed by three 5 minute washes using TBST. The membrane was developed using Immobilon Forte Western HRP substrate (Millipore) and imaged chemiluminescently using the Amersham Imager.

Nucleotide exchange assay

Biotinylated proteins were diluted to 0.5 µM for SOS1-B and 1 µM for SOS2-B in nucleotide exchange buffer supplemented with 0.4 mM GTP. These samples were run alongside $SOS1^{cat}$, $SOS2^{cat}$, KRasmGDP, KRasmGDP-GTP and background controls, as described in section 2.7.

2.10 Phage display

The 1-loop and 2-loop Affimer libraries were screened against SOS2-B with two screens; cross-reactive and selective (table 6). The cross-reactive screen screened against $SOS2^{cat}$ in panning rounds 1 and 2, and against $SOS1^{cat}$ in panning round 3. The selective screen screened against $SOS2^{cat}$ in all three panning rounds, with deselection against $SOS1^{cat}$ occurring in pre-panning rounds 2 and 3. Assay buffer, used for washes and diluting 10X blocking buffer, varied between screens, with NHS biotinylated targets screened in PBST (phage display 1), while HPDP biotinylated targets were screened in nucleotide exchange buffer (phage display 2).

Round	Pre-panning		Panning	
	Cross-reactive	Selective	Cross-reactive	Selective
1	-	-	SOS2-B	SOS2-B
2	-	SOS1-B	SOS2-B	SOS2-B
3	-	SOS1-B	SOS1-B	SOS2-B

Table 6: Immobilised proteins present in each round of pre-panning and panning of phage display. In panning round 3, both SOS1-B and SOS2-B are present in separate wells, one for screening and the other as a control, alongside the blank control.

For round 1, SOS2-B was immobilised to the panning well of a Streptavidin-coated HBC 8-well strip (Thermo Scientific), while phage from the 1-loop and 2-loop libraries were pre-panned against three blank wells, one after the other. Pre-panned phage were then incubated in the panning well for 2 hours on shaker. Phage were eluted with 0.2 M glycine pH 2.2, followed by elution with triethylamine (Sigma-Aldrich) diluted with PBS to 0.014%, both neutralised with 1 M Tris-HCl pH 9.1 and 1 M Tris-HCl pH 7, respectively. Eluted phage were amplified by inoculation into ER2738 *E. coli* cells. Inoculated cells were plated onto LB-carb plates and incubated overnight at 37°C. Cells were scraped into 2TY media containing 100 µg/mL carbenicillin (2TY-carb) and infected with M13K07 helper phage. Following 30 minutes incubation at 37°C with shaking at 90 rpm, 16 µL 30 mg/mL kanamycin was added for overnight incubation at 25°C with shaking at 170 rpm. Phage were precipitated with PEG-NaCl (10% (w/v) PEG 8000, 2.5 M NaCl) and TE buffer (10 mM Tris, 1 mM EDTA) for storage.

For round 2, Dynabeads® MyOne™ Streptavidin T1 beads (Invitrogen) were immobilised with SOS2-B for panning rounds of both screens and SOS1-B for two lots of pre-panning of the selective screen. A 125 µL aliquot of phage from panning round 1 was added to pre-panning rounds for both screens. Pre-panned phage were added to panning beads, with 1 µg $SOS1^{cat}$ added to the selective screen. Phage were panned on KingFisher Flex with the

"Phage_Display_Competition" protocol (table 7) and then incubated for 24 hours with final concentrations of 2X blocking buffer, 16% glycerol (Sigma-Aldrich), 1X Halt™ protease inhibitor cocktail and 1 µg $SOS2^{cat}$ for competitive binding. Phage were then eluted into 0.2 M glycine pH 2.2 and diluted triethylamine on KingFisher Flex with the "Phage_Display_Wash_Elute" protocol (table 7) and neutralised with 1 M Tris-HCl pH 9.1 and 1 M Tris-HCl pH 7, respectively. Eluted phage were amplified and precipitated as described above.

"Phage_Display_Competition" protocol		
Step	**Plate**	**Details**
Pick up tip comb	Tip comb	
Collect beads	Binding plate	Collect beads
Binding	Binding plate	Release beads, 10 seconds fast mix, 1 minute slow mix, collect beads
Wash 1	Wash 1 plate	Release beads, 1 minute slow mix, collect beads
Wash 2	Wash 2 plate	Release beads, 1 minute slow mix, collect beads
Wash 3	Wash 3 plate	Release beads, 1 minute slow mix, collect beads
Wash 4	Wash 4 plate	Release beads, 1 minute slow mix, collect beads
Particle release	Elution plate	Release beads
Leave tip comb	Tip comb	
"Phage_Display_Wash_Elute" protocol		
Step	**Plate**	**Details**
Pick up tip comb	Tip comb	
Collect beads	Binding plate	Collect beads
Binding	Binding plate	Release beads, 10 seconds fast mix, collect beads
Wash 1	Wash 1 plate	Release beads, 1 minute slow mix, collect beads
Wash 2	Wash 2 plate	Release beads, 1 minute slow mix, collect beads
Wash 3	Wash 3 plate	Release beads, 1 minute slow mix, collect beads
Wash 4	Wash 4 plate	Release beads, 1 minute slow mix, collect beads
pH elution	Glycine pH 2.2 plate	Release beads, 7.5 minutes fast mix, 5 seconds bottom mix, collect beads
Triethylamine elution	Triethylamine plate	Release beads, 3.5 minutes slow mix, 5 second bottom mix, collect beads
Leave tip comb	Tip comb	

Table 7: KingFisher Flex protocols for phage display. Details of the "Phage_Display_Competition" and "Phage_Display_Wash_Elute" protocols used for phage display.

For round 3, NeutrAvidin-coated HBC 8-well strips (Thermo Scientific) were immobilized with SOS1-B and SOS2-B for panning rounds, as well as leaving a blank well as a control, and SOS1-B

for four wells of pre-panning rounds of the selective screen. For phage display 1, a 100 µL aliquot of phage from panning round 2 was added to pre-panning rounds for both screens, while a 200 µL aliquot of phage was used for phage display 2. Following the final pre-panning round, phage volume was increased to 300 µL with 2X blocking buffer, with 1 µg $SOS1^{cat}$ added to the selective screen. Phage were divided between $SOS2^{cat}$, $SOS1^{cat}$ and blank panning wells and incubated for 30 minutes on shaker. Panning wells were washed and 2X blocking buffer, 80% glycerol, 100X Halt™ protease inhibitor cocktail and 2 µg $SOS2^{cat}$ added to all wells for 24 hours of incubation at room temperature on shaker. Phage were eluted as described for round 1 and inoculated into ER2738 *E. coli* cells. Cells were plated on LB-carb plates in a range of volumes from 0.01 µL to 10 µL for the $SOS1^{cat}$ well of cross-reactive screen and the $SOS2^{cat}$ well of selective screen, as well as at 10 µL for all other panning wells, and incubated overnight at 37°C. The number of colonies on the 10 µL plates were counted or estimated for all panning wells. Single colonies were picked from the $SOS1^{cat}$ plates of the cross-reactive screen and the $SOS2^{cat}$ plates of the selective screen into 100 µL 2TY-carb in a 96-well plate and incubated for 5 hours at 37°C with shaking at 1050 rpm with breathable seal. A 50 µL aliquoted of phage was taken and added to 100 µL fresh 2TY-carb and stored at 4°C for sequencing. A 20 µL aliquoted was taken and added to 200 µL fresh 2TY-carb in a deep-well plate and incubated for 1 hour at 37°C with shaking at 1050 rpm. Phage were then infected with M13K07 helper phage, followed by kanamycin, as described above, for phage ELISAs.

2.11 Phage ELISA

The assay buffer used for phage display was used for washes and dilution of 10X blocking buffer for phage ELISA. F96 MaxiSorp™ Nunc-Immuno plates (Thermo Scientific) were coated with 50µL 5 µg/mL Streptavidin (Life Technologies) and incubated for 4 hours at room temperature on shaker. Following incubation, 100 µL 3X blocking buffer was added to wells and incubated overnight at 37°C.

Plates were washed once with assay buffer and 50 µL SOS2-B diluted 1:500 in 2X blocking buffer added to 4 columns, 50 µL SOS1-B diluted 1:500 in 2X blocking buffer added to 4 columns, and 50 µL 2X blocking buffer added to 4 columns as blank negative controls. Plates were incubated for 1 hour at room temperature on shaker. Plates were washed once and 10 µL 10X blocking buffer added to all wells. A deep-well plate containing phage was centrifuged for 10 minutes at 3000 rpm and 40 µL supernatant containing phage aliquoted to each section: $SOS2^{cat}$, $SOS1^{cat}$ and blank. Plates were incubated for 1 hour at room temperature on a shaker. Plates were washed once and 50 µL anti-Fd-bacteriophage-HRP (Seramun Diagnostica) diluted 1:1000 in 2X blocking buffer added to all wells. Plates were incubated for 1 hour at room temperature on shaker. Plates were washed 10 times and 50 µL SeramunBlau® fast TMB/substrate solution was

added to all wells. Plates were allowed to develop on shaker, following which A_{620} was measured and photographs taken.

2.12 Sequencing of Affimer reagents following phage display

Phage display 1

Affimer reagents with no background binding (A_{620} < 0.05 in blank control of phage ELISA) were selected for sequencing from phage display 1. These Affimer reagents were sent off for sequencing via stabbing pipette tips, dipped into selected phage wells, into 96-well plate with LB agar containing 100 µg/mL carbenicillin. The plate was sent to Genewiz for Sanger Sequencing using the M13R universal primer (5'-CAGGAAACAGCTATGAC-3'). Equal volumes of 30% glycerol were added to the remaining phage to make a glycerol stock plate and frozen at -80°C for storage.

Phage display 2

Affimer reagents with no background (A_{620} < 0.05 in blank control) and selective for $SOS2^{cat}$ (A_{620} < 0.1 in $SOS1^{cat}$) were selected for sequencing from phage display 2. Overnight cultures were prepared from these Affimer reagents with 1 µL phage added to 4 mL 2TY-carb. Equal volumes of 30% glycerol were added to the remaining phage to make a glycerol stock plates and frozen at -80°C for storage.

Following overnight incubation, cells were centrifuged at 4000 *x*g for 5 minutes. The supernatant was poured off and plasmid DNA extracted from pellets using a QIAprep Spin Miniprep kit, following the manufacturer's instructions. Nuclease free water was used to elute the DNA and A_{260} measured to determine DNA concentration. pDHis plasmid DNA was then sent off to Genewiz for Sanger Sequencing using the M13R universal primer.

2.13 JM83 protein production and purification of His-tagged Affimer reagents from phage display 1

Selected Affimer reagents were spread onto LB-carb plates via scratching frozen wells of glycerol stock plate with pipette tip. LB-carb plates were incubated overnight at 37°C. A single colony was picked for each Affimer reagent and placed in 5 mL LB broth containing 100 µg/mL carbenicillin in a 50 mL falcon tube. This was incubated overnight at 37°C with shaking at 230 rpm. Cells were centrifuged at 4000 *x*g for 5 minutes. Supernatant was poured off and pDHis plasmid DNA extracted from pellets using a QIAprep Spin Miniprep kit, following the

manufacturer's instructions. Nuclease free water was used to elute the DNA and A_{260} measured to determine the concentration.

Plasmid DNA was transformed into JM83 chemically competent *E. coli* cells, as described in section 2.1. Following overnight incubation, a single colony was picked for each Affimer reagent and placed into terrific broth (TB) autoinduction media with trace elements (Formedium) supplemented with 100 µg/mL carbenicillin (TB-carb) aliquoted in a deep-well plate. The plate was covered with a breathable seal and incubated for 6 hours at 37°C with shaking at 1050 rpm. The day cultures were used to inoculate 50 mL TB-carb in 250 mL flasks. These flasks were incubated for 72 hours at 25°C with shaking at 250 rpm. After 48 hours, cultures were induced with a 0.1 mM final concentration of IPTG. Following 72 hours, cells were harvested by centrifugation for 20 minutes at 4000 *x*g. The supernatant poured off and pellets frozen at -20°C.

Cell pellets were thawed and resuspended in 3 mL Affimer lysis buffer (table 3) supplemented with 0.1 mg/mL Lysozyme®, 1% Triton™ X-100, 10 U/mL Benzonase® Nuclease and 1X Halt™ protease inhibitor cocktail. Cell-lysis buffer mixture was transferred to 15 mL falcon tube and incubated for 1 hour at room temperature on a rotator, followed by heat denaturation by incubation at 50°C for 20 minutes. Heat denatured protein was centrifugated for 20 minutes at 4800 *x*g to obtain lysate. Meanwhile, His Mag Sepharose Ni magnetic beads (GE Healthcare) were prepared by washing 150 µL slurry per sample with Affimer wash buffer (table 3). Beads were resuspended in 50 µL wash per sample.

Lysate was distributed between 3 deep 96-well plates, with 950 µL per well of the binding plates. To the first binding plate, 50 µL beads was added per well. Three wash plates were prepared with 1 mL Affimer wash buffer (table 3) per well in a deep 95-well plate. The elution plate was prepared with 150 µL nucleotide exchange buffer supplemented with 500 mM imidazole per well in 96-well plate.

Plates and tip comb were loaded into KingFisher Flex and the "chris_protein_purification" protocol started (table 8). Following the protocol, eluted proteins in elution plate were transferred to 1.5 mL Protein LoBind tubes (Eppendorf) and stored overnight at 4°C.

"chris_protein_purification" protocol		
Step	**Plate**	**Details**
Pick up tip comb	Tip comb	
Collect beads	Binding plate	Collect beads
Binding 1	Lysate 1 plate	Release beads, 60 minutes slow mix, collect beads
Binding 2	Lysate 2 plate	Release beads, 60 minutes slow mix, collect beads
Binding 3	Lysate 3 plate	Release beads, 60 minutes slow mix, collect beads
Wash 1	Wash 1 plate	Release beads, 5 minutes slow mix, collect beads
Wash 2	Wash 2 plate	Release beads, 5 minutes slow mix, collect beads
Wash 3	Wash 3 plate	Release beads, 5 minutes slow mix, collect beads
Elution	Imidazole	Release beads, 20 minutes slow mix, collect beads
Leave tip comb	Tip comb	

Table 8: KingFisher Flex protocol for JM83 protein purification. Details of the "chris_protein_purification" protocol used for JM83 protein purification.

Affimer proteins were aliquoted into Pur-A-Lyzer™ mini dialysis tubes and dialysed into nucleotide exchange buffer for 4 hours at 4°C, with two buffer changes. Affimer proteins were then centrifuged for 2 minutes at 20000 *x*g. The A_{280} of the Affimer proteins was measured and concentration determined using the extinction co-efficients. Affimer proteins were diluted with nucleotide exchange buffer to make stock concentrations of 12 µM and stored at 4°C to be used within the week for nucleotide exchange assays in section 2.7.6.

2.14 Statistical Analysis

Statistical analysis was performed using one-way and two-way ANOVA with multiple comparisons on GraphPad Prism 8. Significant differences between the SOS control and the test groups were defined with p values of less than 0.05 (*), less than 0.005 (**), less than 0.001 (***) and less than 0.0001 (****), or more than 0.05 for not significant (ns). These were included on the graphs. Error bars are ± standard deviation (SD) of either the technical repeats where n = 1, or of the biological repeats where n = 4.

3. Results

3.1 Establishment of the SOS1^{cat} catalysed nucleotide exchange assay

The aim of this thesis is to isolate and characterise SOS2 binding Affimer reagents. Inhibitors of the catalytic domain of SOS2 can then be used, alongside inhibitors of the catalytic domain of SOS1, to study the effects of SOS inhibition on downstream signalling in Ras mediated cancer signalling pathways.

Inhibition of SOS can be measured in a biochemical assay called nucleotide exchange, via measuring a decrease in the initial rate of nucleotide exchange of GDP to GTP on Ras (figure 8). In the absence of inhibitors, mant-GDP (mGDP) loaded KRas is exchanged for GTP in the presence of SOS. Release of mGDP into buffer quenches its fluorescence. Inhibition of SOS binding to KRas by Affimer reagents decreases exchange of mGDP for GTP and therefore keeps fluorescent levels higher, and a slower initial rate. In the absence of SOS, intrinsic nucleotide exchange, the exchange of mGDP for GTP on KRas, occurs at a much slower rate.

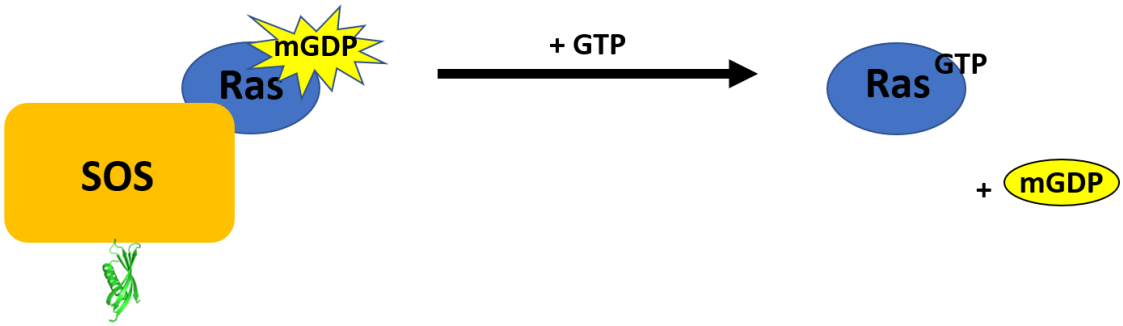

Figure 8: Schematic model of the nucleotide exchange assay with Affimer reagents inhibiting SOS. KRas is loaded with mGDP, which fluorescence at 440 nm following excitation at 365 nm. SOS, whether SOS1 or SOS2, catalyses exchange of mGDP for GTP, which releases mGDP into the buffer causing its fluorescence to be quenched, which can be measured using a plate reader. Inhibition of SOS, such as by Affimer reagents (green), will cause decreased exchange of mGDP for GTP. In the absence of SOS, intrinsic nucleotide exchange continues to occur albeit at a slower rate.

Initially recombinant proteins needed to be purified to set up the nucleotide exchange assay. The plasmids encoding the DNA for the catalytic domain of SOS1 (SOS1^{cat}) and KRas were transformed into XL-1 Blue *E. coli* cells, colonies picked and grown in 5 mL of LB media overnight

and were purified (sections 2.1 and 2.2). Plasmids were verified using sequencing via Sanger Sequencing with the universal T7 primer.

After verification of sequence, the plasmids were transformed into BL21 (DE3) *E. coli* cells, colonies picked and grown in 400 mL cultures to produce protein (sections 2.1 and 2.3). Proteins were purified using Ni-NTA resin. To confirm the protein was being produced and to check the purity, samples were collected during extraction and purification and run on a 15% SDS-PAGE and stained with Coomassie blue (figures 9A and 9B). Bands indicating protein were present at the expected molecular weights of 59.3 kDa for $SOS1^{cat}$ and 21.7 kDa for KRas (indicated by arrows). Purified $SOS1^{cat}$ was then dialysed to remove imidazole (section 2.5) and KRas was loaded with mGDP (section 2.6). Previously, mGDP loading via this protocol was confirmed by native mass-spectrometry by Dr Kevin Tipping. The concentrations of both $SOS1^{cat}$ and KRasmGDP were determined using a BCA protein assay kit (figures 9C and 9D).

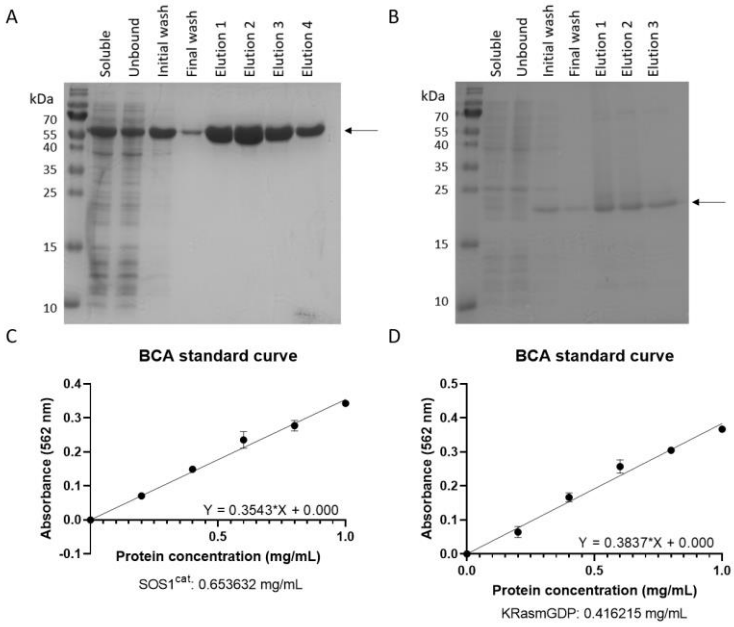

Figure 9: Production and purification of $SOS1^{cat}$ and KRas protein. Following production of (A) $SOS1^{cat}$ and (B) KRas in BL21 (DE3) *E. coli* cells, samples were taken during protein extraction and purification, which were run on a 15% SDS-PAGE and stained with Coomassie blue. Arrows indicate protein at the expected molecular weights. Purified protein concentrations were determined using a BCA protein assay kit, with standards and protein samples of (C) $SOS1^{cat}$ and (D) KRasmGDP measured at 562 nm. Error bars ± SD.

3.2 Affimer s18 shows nanomolar IC_{50} value in the $SOS1^{cat}$ catalysed nucleotide exchange assay

Previously, Affimer reagents have been isolated that inhibit $SOS1^{cat}$ *in vitro* and in cells but showed cross-reactivity to $SOS2^{cat}$. Here, the initial aim was to characterise the inhibition of $SOS1^{cat}$ by a cross-reactive Affimer reagents, Affimer s18, by performing an IC_{50} curve to determine potency.

Affimer s18 protein was produced and purified to determine its effect on nucleotide exchange. The plasmid encoding the DNA for Affimer s18 was transformed into XL-1 Blue *E. coli* cells, a colony picked and grown in 5 mL of LB media overnight and was purified (sections 2.1 and 2.2). The plasmid was verified using sequencing via Sanger Sequencing with the universal T7 primer.

After verification of sequence, the plasmid was transformed into BL21 (DE3) *E. coli* cells, colonies picked and grown in 50 mL cultures to produce protein (sections 2.1 and 2.3). Protein was purified using Ni-NTA resin. To confirm the protein was being produced and to check the purity, samples were collected during extraction and purification and run on a 15% SDS-PAGE and stained with Coomassie blue (figure 10A). Bands indicating protein were present at the expected molecular weights of 12.6 kDa (indicated by an arrow). Directly prior to use, Affimer s18 was dialysed into assay buffer and its concentration determined using the extinction co-efficient and measurement of A_{280}.

To understand the potency of Affimer s18 against $SOS1^{cat}$, the IC_{50} value, which gives the half maximal inhibitory concentration, needed to be determined. A titration of Affimer s18 was tested in the nucleotide exchange assay against $SOS1^{cat}$, initial rates calculated, and results analysed using Origin Pro (section 2.7.2). Analysis gave an IC_{50} value with standard error of the mean of 176.2 nM ± 9.92 (figure 10B). This means 176.2 nM Affimer s18 is required to inhibit 0.25 µM $SOS1^{cat}$ by 50% in a biochemical assay. This value can be used to compare the potency of different Affimer reagents for the same target. The curve also demonstrates that at high concentrations of Affimer s18, nucleotide exchange is inhibited to levels of intrinsic nucleotide exchange (denoted by the line).

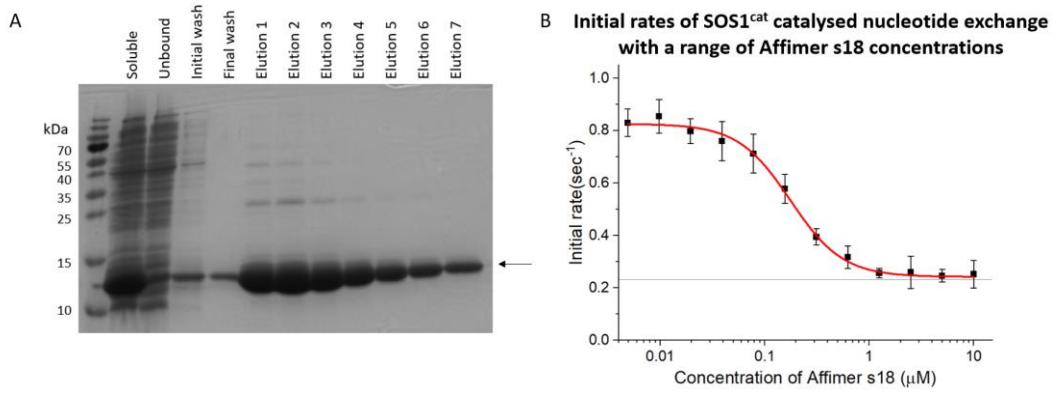

Figure 10: Production and purification of Affimer s18 and IC_{50} curve. (A) Following production of Affimer s18 in BL21 (DE3) *E. coli* cells, samples were taken during protein extraction and purification, which were run on a 15% SDS-PAGE and stained with Coomassie blue. The arrow indicates protein at the expected molecular weight. (B) Potency of Affimer s18 against $SOS1^{cat}$ catalysed nucleotide exchange was determined using an IC_{50} curve of Affimer s18 concentrations against initial rates of $SOS1^{cat}$ catalysed nucleotide exchange. Line denotes KRasmGDP-GTP, the initial rate of intrinsic nucleotide exchange in the absence of $SOS1^{cat}$ and inhibitors from two biological repeats. Results represent four biological repeats (n = 4), two of which were performed by Sophie Saunders. Error bars are ± SD.

3.3 Alanine scanning of Affimer s18 identified key residues for inhibition of $SOS1^{cat}$

Next, Affimer s18 was further characterised using alanine scanning to identify key residues in the VRs of the Affimer that are important for nucleotide exchange. This will help determine the key structural and physical properties of the interaction important for inhibition.

Affimer s18 has two 9 amino acid VRs; VR 1 and VR 2. These 18 residues were individually mutated to alanine (table 9) to test in the $SOS1^{cat}$ catalysed nucleotide exchange assay.

Affimer s18	VR 1	VR 2	Affimer s18	VR 1	VR 2
WT	TSERWPHFD	QDRYPSYIW	WT	TSERWPHFD	QDRYPSYIW
1.1	**A**SERWPHFD	QDRYPSYIW	2.1	TSERWPHFD	**A**DRYPSYIW
1.2	T**A**ERWPHFD	QDRYPSYIW	2.2	TSERWPHFD	Q**A**RYPSYIW
1.3	TS**A**RWPHFD	QDRYPSYIW	2.3	TSERWPHFD	QD**A**YPSYIW
1.4	TSE**A**WPHFD	QDRYPSYIW	2.4	TSERWPHFD	QDR**A**PSYIW
1.5	TSER**A**PHFD	QDRYPSYIW	2.5	TSERWPHFD	QDRY**A**SYIW
1.6	TSERW**A**HFD	QDRYPSYIW	2.6	TSERWPHFD	QDRYP**A**YIW
1.7	TSERWP**A**FD	QDRYPSYIW	2.7	TSERWPHFD	QDRYPS**A**IW
1.8	TSERWPH**A**D	QDRYPSYIW	2.8	TSERWPHFD	QDRYPSY**A**W
1.9	TSERWPHF**A**	QDRYPSYIW	2.9	TSERWPHFD	QDRYPSYI**A**

Table 9: Alanine scanning sequences of Affimer s18. VRs of wild-type (WT) Affimer s18 and Affimer s18 alanine mutants, denoted by position in VR. Bold denotes the mutated alanine residues.

Affimer s18 was mutated using QuikChange site-directed mutagenesis with an annealing temperature of 72°C (section 2.8). All alanine mutants, except 2.3 and 2.8, produced DNA product visualised on a 1% agarose gel (figure 11A). Since no product was seen for mutants 2.3 and 2.8, an annealing temperature gradient from 60 to 72°C was carried out to troubleshoot. Both mutants produced product at all temperatures, as visualised on a 1% agarose gel, with 70°C for mutant 2.3 and 63°C for mutant 2.8 determined to be optimal due to the darkest bands indicating the presence of the most product (figure 11B).

All mutated DNA products were transformed into XL-1 Blue *E. coli* cells, colonies picked and grown in 5 mL of LB media overnight and were purified (sections 2.1 and 2.2). The plasmids were sequenced via Sanger Sequencing with the universal T7 primer. All mutants, except 1.1 and 1.2, returned correctly mutated sequences. Mutants 1.1 and 1.2 were produced again via site-directed mutagenesis with an annealing temperature of 72°C, and the products were visualised on a 1% agarose gel (figure 11C). Repeat transformation and purification of mutants 1.1 and 1.2 DNA products, followed by sequencing via Sanger Sequencing with the universal T7 primer, indicated site-directed mutagenesis was successful in producing all 18 alanine mutants required for alanine scanning.

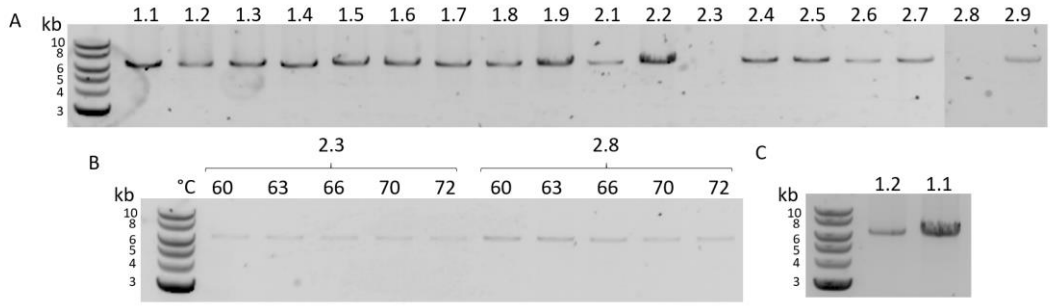

Figure 11: Site-directed mutagenesis of Affimer s18 for alanine scanning. Following site-directed mutagenesis and *DpnI* digest, products were mixed with orange G loading dye, run on 1% agarose gel and imaged. Annealing temperatures varied, with (A) all alanine mutants initially mutated at an annealing temperature of 72°C, (B) repeat of alanine mutants 2.3 and 2.8 with an annealing heat temperature gradient, and (C) repeat of alanine mutants 1.1 and 1.2 at an annealing temperature of 72°C.

Following successful site-directed mutagenesis, all Affimer s18 alanine mutant plasmids were transformed into BL21 (DE3) *E. coli* cells, colonies picked and grown in 50 mL cultures to produce protein (sections 2.1 and 2.3). Proteins were purified using Ni-NTA resin. To confirm the protein was being produced and to check the purity, samples were collected during extraction and purification of Affimer s18 alanine mutant 1.1 (figure 12A), as well as from the first elution collected for the other Affimer s18 alanine mutants (figures 12B and 12C) and run on a 15% SDS-PAGE and stained with Coomassie blue. Bands indicating protein were present at the expected molecular weight of 12.6 kDa (indicated by arrows).

Fainter bands were also observed around 25 kDa, which are visible due to overloading of the SDS-PAGE with sample. These may be caused by incomplete denaturation of protein during heating or re-folding prior to loading of samples. Given more time, the state of the Affimer proteins would have been checked using size-exclusion chromatography, to confirm they were monomers. Directly prior to use, Affimer s18 alanine mutants were dialysed into assay buffer and their concentrations determined using the extinction co-efficient and measurement of A_{280}.

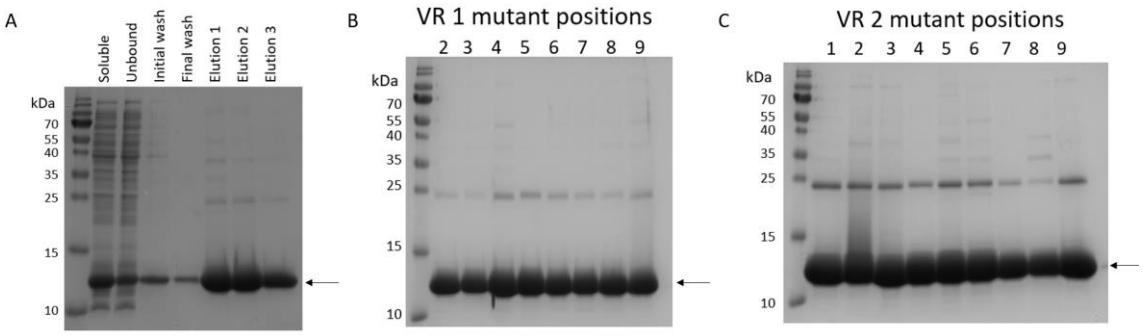

Figure 12: Production and purification of Affimer s18 alanine mutants. Following production of Affimer s18 alanine mutants in BL21 (DE3) *E. coli* cells, samples were taken during protein extraction and purification, which were run on a 15% SDS-PAGE and stained with Coomassie blue. (A) All samples taken were run for Affimer s18 1.1 alanine mutant, while elution 1 samples were run for (B) Affimer s18 VR 1 alanine mutants and (C) Affimer s18 VR 2 alanine mutants. Arrows indicate protein at the expected molecular weight.

To determine the effects of individual residues on $SOS1^{cat}$ inhibition, all 18 Affimer s18 alanine mutant proteins were tested in the nucleotide exchange assay against $SOS1^{cat}$ (section 2.7.3). A final Affimer concentration of 5 µM was used as it was a concentration at which WT Affimer s18 demonstrated its maximal inhibition of $SOS1^{cat}$ (figure 10B).

Of the 18 mutated residues, alanine mutations of five residues individually prevented Affimer s18 from inhibiting $SOS1^{cat}$, shown by increases in initial rates of nucleotide exchange to levels observed in the negative control, $SOS1^{cat}$ (figure 13). The residues 1.4 arginine, 1.6 proline, 1.7 histidine, 2.2 aspartate and 2.4 tyrosine, therefore, must be important for binding of Affimer s18 to $SOS1^{cat}$ or inhibition of $SOS1^{cat}$. However, as this experiment was only performed twice for VR 1 mutants and once for VR 2 mutants, further repeats are required to perform statistical analysis and validate the results.

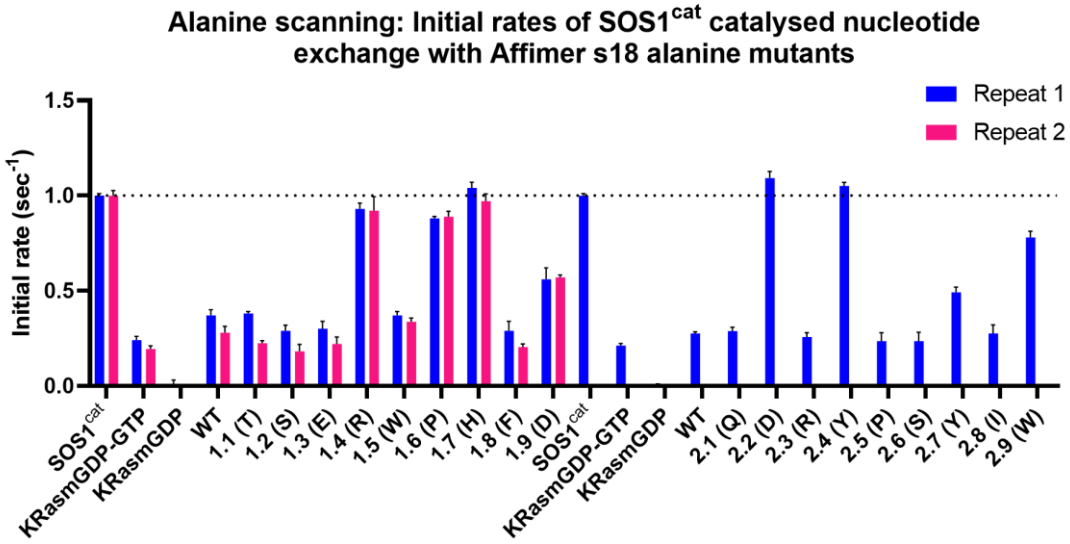

Figure 13: Effects of alanine scanning Affimer s18 mutants on initial rates of SOS1^{cat} catalysed nucleotide exchange. Alanine scanning Affimer s18 mutants, denoted as position in VR and single letter code of mutated amino acid, at 5 µM were assayed against SOS1^{cat} catalysed nucleotide exchange. WT Affimer s18 was used as a positive control and KRasmGDP-GTP demonstrates the initial rate of intrinsic nucleotide exchange in the absence of SOS1^{cat} and inhibitors. Initial rates of nucleotide exchange were normalised to SOS1^{cat} and KRasmGDP controls. Dashed line denotes initial rate of normalised SOS1^{cat} control. Results represent two biological repeats (n = 2) for VR 1 and one biological repeat (n = 1) for VR 2. Error bars are ± SD.

3.4 Optimisation of SOS2^{cat} protein expression

In order to investigate the role of SOS2 in Ras mediated cancer signalling, Affimer reagents needed to be isolated against the catalytic domain of SOS2 (SOS2^{cat}). Initially, protein production of SOS2^{cat} was optimised.

To produce SOS2^{cat}, the plasmid encoding the DNA for SOS2^{cat} was transformed into XL-1 Blue *E. coli* cells and the plasmid purified (sections 2.1 and 2.2). The plasmid was sequenced via Sanger Sequencing with the universal T7 primer. The sequences of His-tagged SOS1^{cat} and SOS2^{cat} used for protein production have 80% sequence identity and 93% sequence similarity, aligned using the Clustal Omega programme on UniProt. This was visualised in BioEdit (figure 14).

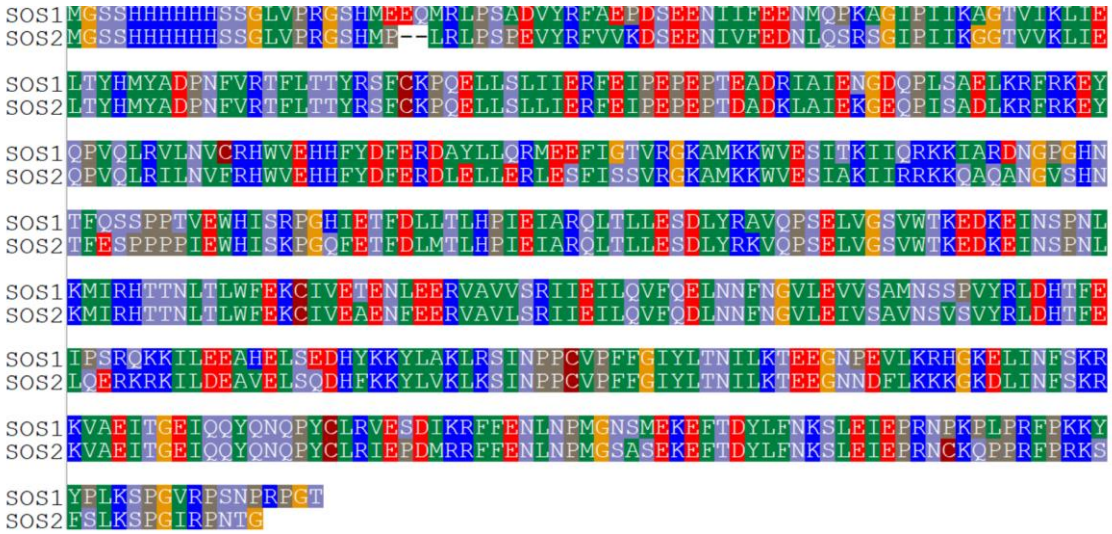

Figure 14: Alignment of the His-tagged catalytic domains of SOS1 and SOS2. The sequences of His-tagged SOS1^{cat} and SOS2^{cat} were aligned in BioEdit for visualisation. Amino acids are categorised by colour according to their properties; green for hydrophobic side chains, grey for uncharged side chains, red for negatively charged side chains, blue for positively charged side chains, orange for glycine, brown for proline, and burgundy for cysteine.

For SOS2^{cat} expression trials, the verified plasmid was transformed into BL21 (DE3) *E. coli* cells, colonies picked and grown in four 50 mL cultures under different conditions to produce protein (sections 2.1 and 2.4). Cultures were induced at OD_{600} of either 0.6 or 0.8, followed by incubation at either 25°C or 30°C, with 1 mL samples taken before induction and following induction after 4 hours, 6 hours and overnight culture time. These samples were lysed, and the soluble fraction run on a 15% SDS-PAGE and stained with Coomassie blue (figure 15A). The strongest band at approximately 58.5 kDa, the molecular weight of SOS2^{cat}, was used to determine the optimal conditions for SOS2^{cat} protein production. Therefore, the optimal SOS2^{cat} protein production conditions are induction at an OD_{600} of 0.8, followed by culture at 30°C for 4 hours.

Using these optimised protein production conditions, the SOS2^{cat} plasmid was transformed into BL21 (DE3) *E. coli* cells, colonies picked and grown in 400 mL culture to produce protein (section 2.1 and 2.3). Protein was purified using Ni-NTA resin. To confirm the protein was being produced and to check the purity, samples were collected during purification and run on a 15% SDS-PAGE and stained with Coomassie blue (figure 15B). Bands indicating protein were present at the expected molecular weight of 58.5 kDa. Purified SOS2^{cat} was dialysed to remove imidazole (section 2.5) and the concentrations of SOS2^{cat} was determined using a BCA protein assay kit (figure 15C).

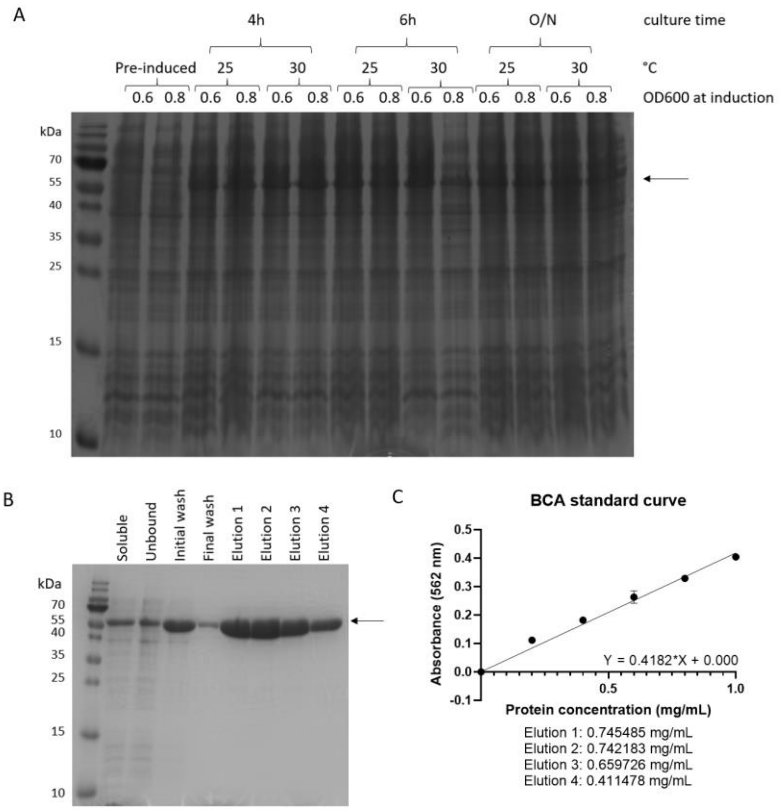

Figure 15: Production and purification of SOS2^{cat}. (A) During SOS2^{cat} expression trials, 1 mL samples were taken of pre-induced and induced cultured BL21 (DE3) *E. coli* cells. These samples were lysed, and the soluble fraction run on a 15% SDS-PAGE and stained with Coomassie blue. The arrow indicates protein at the expected molecular weight. (B) Following production of SOS2^{cat} in BL21 (DE3) *E. coli* cells at optimal conditions, samples were taken during protein extraction and purification, which were run on a 15% SDS-PAGE and stained with Coomassie blue. The arrow indicates protein at the expected molecular weight. (C) Purified SOS2^{cat} protein concentration was determined using a BCA protein assay kit, with standards and protein samples measured at 562 nm. Error bars are ± SD.

3.5 Optimisation of the SOS2^{cat} catalysed nucleotide exchange assay, validated by Affimer s18 inhibition of SOS2^{cat}

Next, the SOS2^{cat} catalysed nucleotide exchange assay needed to be optimised so Affimer reagents isolated against SOS2^{cat} can be tested for their ability to inhibit the function of SOS2^{cat}. This also demonstrated that SOS2^{cat} is functional in catalysing nucleotide exchange which is important when isolating Affimer reagents. To optimise the SOS2^{cat} catalysed nucleotide exchange assay, a range of SOS2^{cat} protein concentrations were tested in the nucleotide exchange assay and compared to the optimised SOS1^{cat} protocol (section 2.7.4).

The initial rates of nucleotide exchange for the different SOS2^{cat} concentrations were normalised to SOS1^{cat} (figure 16A). A final concentration of 0.5 µM SOS2^{cat} produced a similar initial rate to the optimised 0.25 µM SOS1^{cat}, as well as a similar curve of fluorescence intensity over time (figure 16B), and therefore was determined as the optimal SOS2^{cat} concentration for the SOS2^{cat} catalysed nucleotide exchange assay. This concentration of SOS2^{cat} is double that of SOS1^{cat}, indicating that SOS2^{cat} is approximately half as active compared to SOS1^{cat} in this nucleotide exchange assay.

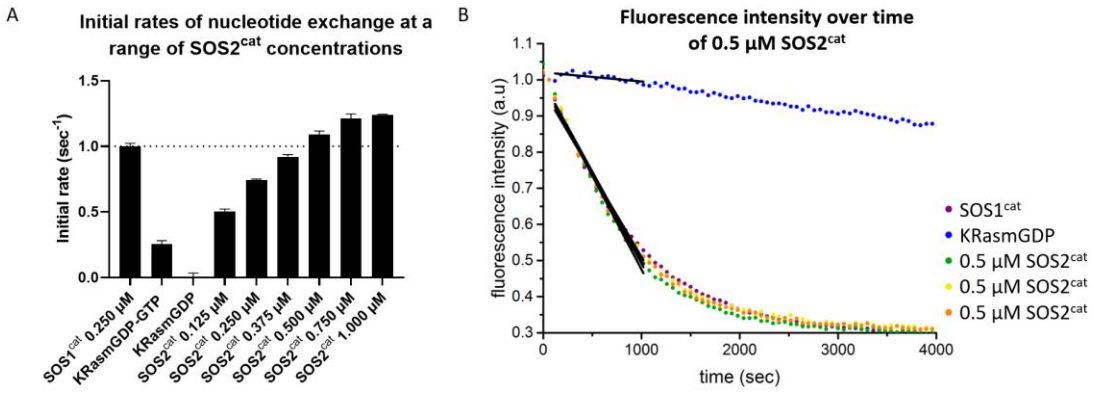

Figure 16: Optimisation of the SOS2^{cat} catalysed nucleotide exchange assay. (A) Initial rates of nucleotide exchange with a range of SOS2^{cat} concentrations. KRasmGDP-GTP demonstrates the initial rate of intrinsic nucleotide exchange in the absence of SOS1^{cat} and inhibitors. Initial rates of nucleotide exchange were normalised to SOS1^{cat} and KRasmGDP controls. Dashed line denotes initial rate of normalised SOS1^{cat} control. Results represent one biological repeat (n = 1). Error bars are ± SD. (B) Graph of normalised fluorescence intensity over time of 0.5 µM SOS2^{cat} (3 repeats) with SOS1^{cat} and KRasmGDP controls, and linear lines used to determine initial rates.

To validate the SOS2^{cat} catalysed nucleotide exchange assay and test Affimer s18's ability to inhibit SOS2^{cat}, a final concentration of 10 µM Affimer s18 was tested in the SOS2^{cat} catalysed nucleotide exchange assay (section 2.7.5). This Affimer concentration is double that used for alanine scanning in order to keep the same Affimer to SOS ratio, as the concentration of SOS2^{cat} is double that used for SOS1^{cat} in the nucleotide exchange assay. At this concentration, Affimer s18 inhibited SOS2^{cat} to an initial rate equivalent to intrinsic nucleotide exchange, indicating Affimer s18 inhibits SOS2^{cat} and that the SOS2^{cat} catalysed nucleotide exchange assay worked (figure 17). Proteins and nucleotide exchange assay results were generated by Sophie Saunders.

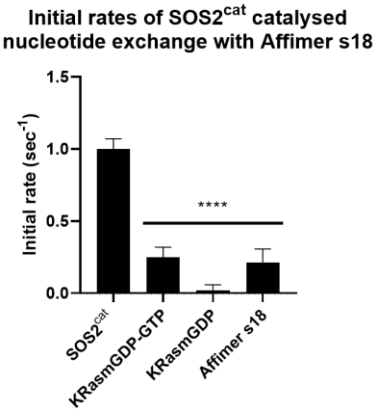

Figure 17: Affimer s18 inhibition of SOS2^{cat} catalysed nucleotide exchange. Initial rates of SOS2^{cat} catalysed nucleotide exchange inhibited by 10 µM Affimer s18. KRasmGDP-GTP demonstrates the initial rate of intrinsic nucleotide exchange in the absence of SOS2^{cat} and inhibitors. Initial rates of nucleotide exchange were normalised to SOS2^{cat} and KRasmGDP controls. Results represent one biological repeat (n = 1). Error bars are ± SD. $p < 0.0001$ (****).

3.6 Phage display 1: Isolation of SOS2^{cat} binding Affimer reagents with NHS biotinylated SOS2^{cat} and SOS1^{cat}

Following optimisation of SOS2^{cat} protein production and of the SOS2^{cat} catalysed nucleotide exchange assay, the functional SOS2^{cat} protein could then be used for phage display to isolate Affimer reagents against SOS2^{cat}. Affimer reagents were isolated via phage display from Affimer phage libraries (figure 18). These libraries are made up of M13 phage expressing Affimer reagents as their pIII coat protein. Each phage expresses Affimer reagents from a singular sequence encoded by the pDHIS phagemid. To isolate SOS2^{cat} binders via phage display, the 1-loop and 2-loop libraries were used. The 2-loop library contains Affimer reagents with two randomised VRs of 9 amino acids each, while the 1-loop library contains Affimer reagents with one randomised VR of 9 amino acids and the second VR containing three AAE repeats, which is unlikely to contribute to binding.

Phage display consists of three rounds of panning of these libraries, with pre-panning occurring before each panning round. Pre-panning can be used to capture Affimer reagents which bind another protein for deselection before panning, first described by Anna Tang [80]. Panning rounds are then used to capture Affimer reagents which bind the target of interest. Those captured in the first panning round are then amplified for the next pre-panning and panning round and repeated again for the third pre-panning and panning round.

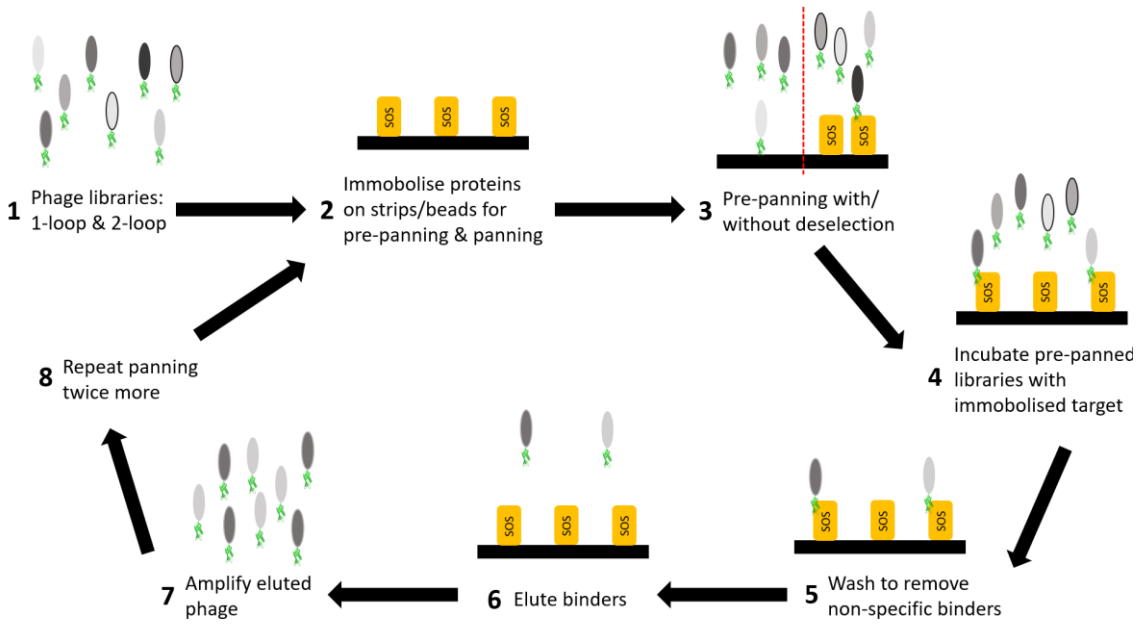

Figure 18: Schematic of phage display. Two phage libraries (grey) expressing Affimer reagents (green) as their pIII coat protein were mixed. Phage express more than one copy of the encoded Affimer reagent; however, this was simplified for the schematic. The biotinylated target, SOS2^{cat}, and deselection protein, SOS1^{cat}, were immobilised on the strip or beads for the pre-panning and panning round. The mixed libraries were then pre-panned with or without SOS1^{cat} deselection. The pre-panned phage were then panned with the immobilised target. Non-specific binders were washed away, and the binders were eluted. The eluted phage were then amplified in ER2738 *E. coli* cells for the next panning round. Following three rounds of panning, individual colonies were tested in phage ELISA and sequenced.

To obtain Affimer reagents against SOS2^{cat}, both selective for SOS2^{cat} and cross-reactive with SOS1^{cat}, phage display was carried out with two screens side-by-side, named selective and cross-reactive. The selective screen was selective for SOS2^{cat} through a deselection of Affimer reagents against SOS1^{cat} in the pre-panning rounds 2 and 3 and selection for SOS2^{cat} binders in all three panning rounds. The cross-reactive screen was completed without deselection, but with selection for SOS2^{cat} binders in panning rounds 1 and 2 and selection for SOS1^{cat} binders in panning round 3.

Since both SOS1^{cat} and SOS2^{cat} were required for phage display, both purified proteins needed to be biotinylated. One method of biotinylating is using EZ-link NHS biotin which labels primary amines (-NH_2), such as the side chain of lysine residues. The catalytic domain of SOS2 contains 38 lysine residues, while the catalytic domain of SOS1 contains 33 lysine residues.

Purified SOS1^{cat} and SOS2^{cat} were biotinylated and then characterised before use (section 2.9) (figure 19). Following biotinylation, BCA protein assays determined the concentration, and ELISAs and western blot analysis validated biotinylation. ELISAs validated the presence of biotin, while western blot analysis validated that the biotinylated proteins were at the expected molecular weights, approximately 59 kDa for SOS1^{cat} and 58 kDa for SOS2^{cat}. Additionally, the biotinylated proteins were tested in the nucleotide exchange assay compared to the unbiotinylated protein form to demonstrate that biotinylation did not ablate nucleotide exchange catalysis activity.

Biotinylated SOS1^{cat}, denoted SOS1-B, came out as half the concentration of biotinylated SOS2^{cat}, denoted SOS2-B. ELISA analysis showed both protein samples contained biotin and western blot analysis of the proteins at the same concentration revealed that both SOS1^{cat} and SOS2^{cat} were biotinylated as expected. There is a slightly thicker band for SOS2-B, which is understandable due to the higher number of lysine residues in SOS2^{cat} compared to SOS1^{cat}. The nucleotide exchange assay of the biotinylated proteins revealed that biotinylation reduced activity of both SOS1^{cat} and SOS2^{cat}, although slightly more for SOS2^{cat}. While there is a statistical significant difference between the initial rates of nucleotide exchange with SOS-B compared to SOS, the initial rates of SOS1-B and SOS2-B are above the KRas intrinsic levels of nucleotide exchange, KRasmGDP-GTP, indicating that even biotinylated, SOS1-B and SOS2-B are still active. Therefore, EZ-link NHS biotinylated SOS1^{cat} and SOS2^{cat} were used for the first phage display screens.

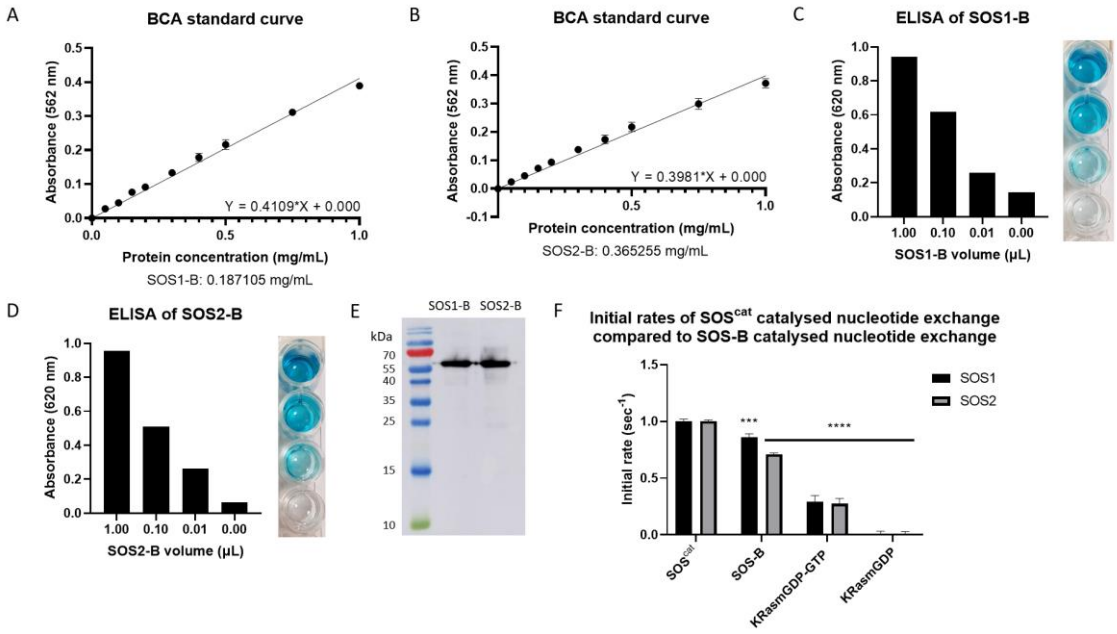

Figure 19: Characterisation of NHS biotinylated SOS1^{cat} and SOS2^{cat}. Biotinylated (A) SOS1^{cat} and (B) SOS2^{cat} protein concentration was determined using a BCA protein assay kit, with standards and protein samples measured at 562 nm. Error bars are ± SD. Biotinylation of (C) SOS1^{cat} and (D) SOS2^{cat} was validated via ELISAs at varying protein volumes, with A_{620} measured and photographs taken. (E) Biotinylation of SOS1^{cat} and SOS2^{cat} was further validated via western blot analysis probed with Streptavidin-HRP. (F) Initial rates of nucleotide exchange of SOS1-B and SOS2-B was compared to the unbiotinylated form. KRasmGDP-GTP demonstrates the initial rate of intrinsic nucleotide exchange in the absence of SOS and inhibitors. Initial rates of nucleotide exchange were normalised to the corresponding SOS isoform and KRasmGDP controls. Results represent one biological repeat (n = 1). Error bars are ± SD. $p < 0.001$ (***), $p < 0.0001$ (****).

Following biotinylation of SOS2^{cat} and SOS1^{cat}, the selective and cross-reactive screens were performed side-by-side (section 2.10). Following three rounds of panning, ER2738 *E. coli* cells were infected with phage and a range of volumes were plated onto LB-carb plates. Following overnight incubation, the number of colonies on plates with 10 µL phage-infected ER2738 *E. coli* cells were counted or calculated from the 1 µL plate (table 10).

Both screens contained a large number of colonies on the blank plates, similar to that observed on the SOS1^{cat} plates. Ideally, colony numbers would be extremely low for the blank plates, as well as on the SOS1^{cat} plate of the selective screen. This would indicate that few phage bound the blank control and SOS1^{cat} control in the third panning round. Nonetheless, colonies were

picked for phage ELISA; 64 from the $SOS2^{cat}$ plates of the selective screen and 32 from the $SOS1^{cat}$ plates of the cross-reactive screen.

Screen	Number of colonies on 10 µL plate		
	$SOS2^{cat}$	$SOS1^{cat}$	Blank
Selective	**155**	14	17
Cross-reactive	1760 (^)	**45**	27

Table 10: Number of colonies present on 10 µL LB-carb plates following phage display 1. Following panning round 3, phage bound to the $SOS2^{cat}$, $SOS1^{cat}$ and blank panning wells were infected into ER2738 *E. coli* cells. Phage-infected cells were plated onto LB-carb plates at a range of volumes, which were incubated overnight at 37°C and the number of colonies on the 10 µL plate counted or calculated from the 1 µL plate as denoted by ^ symbol. Bold denotes the plates from which colonies were picked for phage ELISA.

The colonies picked were tested in phage ELISA against $SOS2^{cat}$, $SOS1^{cat}$ and blank control (section 2.11). The colonies were named and numbered, with S1 denoting Affimer reagents picked from the selective screen, while C1 denoting those from the cross-reactive screen. Of the 96 colonies tested in phage ELISA, 35 phage displayed binding to $SOS2^{cat}$ and no binding to the blank well, defined as an A_{620} below 0.05 (figure 20). From these 35, seven were categorised as $SOS2^{cat}$ selective due to an A_{620} below 0.05 in the $SOS1^{cat}$ well, while the other 28 were categorised as cross-reactive binders. These did not necessarily come from the expected screen, i.e. selective Affimer reagents from the selective screen and cross-reactive Affimer reagents from the cross-reactive screen. This indicated that the screening process was not strict in isolating selective or cross-reactive Affimer reagents, but a combination. Additionally, the high number of Affimer reagents which bound the blank well indicated that the screens did not work well but were still able to isolate $SOS2^{cat}$ binders.

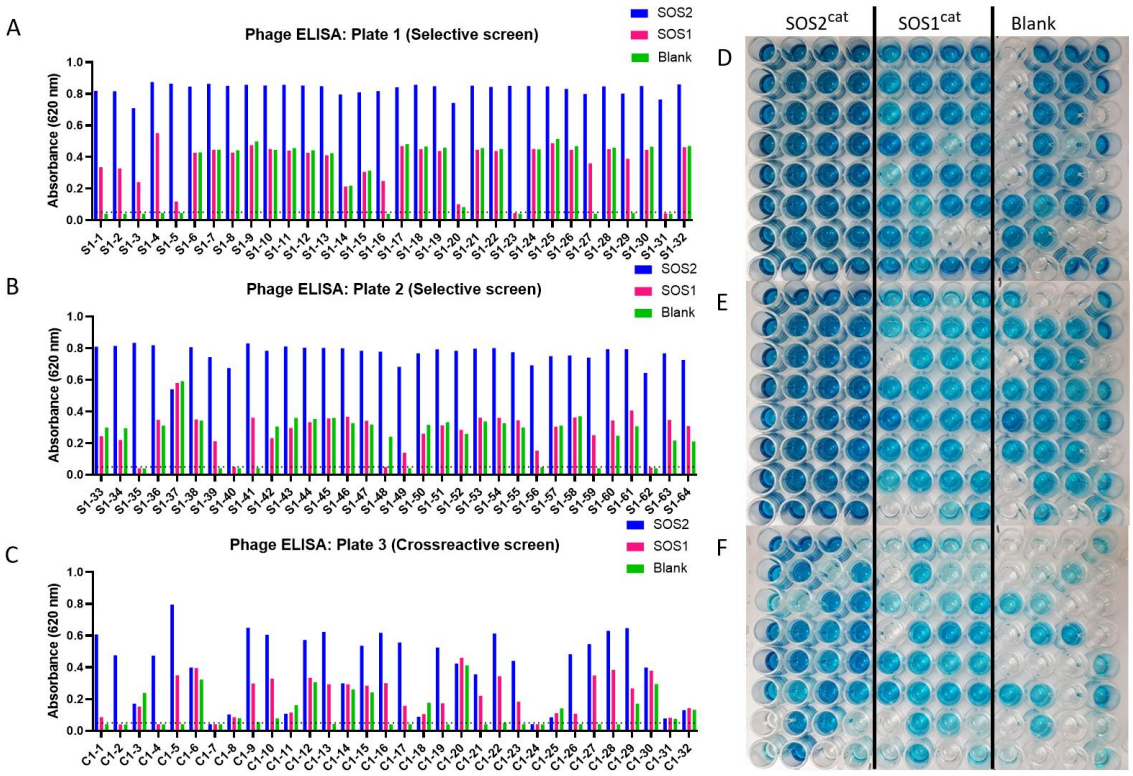

Figure 20: Phage ELISA from phage display 1. From the phage-infected ER2738 *E. coli* cells plated onto LB-carb plates, 96 colonies were picked, and the phage amplified; 64 from the selective screen and 32 from the cross-reactive screen. These were then tested in phage ELISA against SOS2^{cat}, SOS1^{cat} and a blank well. (A-C) Phage ELISA plates were measured at A_{620}. Raw results were graphed with line A_{620} = 0.05 denoting background levels. (D-F) These phage ELISA plates were also photographed for visualisation.

The 35 Affimer reagents selected following phage ELISA were sequenced using the universal M13R primer (section 2.12). From the 35 sequences, 32 contained single peaks in their traces and thus were sequenced correctly. From the 32 sequences, 7 were unique selective Affimer reagents, as demonstrated in the phage ELISA, while 25 demonstrated cross-reactive characteristics in the phage ELISA, with 16 being unique sequences (figure 21).

There are few similarities between the unique Affimer reagents, except that they all have a hydrophobic residue in position 2.9 and the majority have a hydrophobic residue in positions 2.2, 2.4 and 2.7. Additionally, there are no clear similarities between these Affimer reagents and Affimer s18, a SOS1^{cat} and SOS2^{cat} inhibitor isolated in the previous SOS1^{cat} phage display screen, except hydrophobic residues in positions 2.4, 2.7 and 2.9.

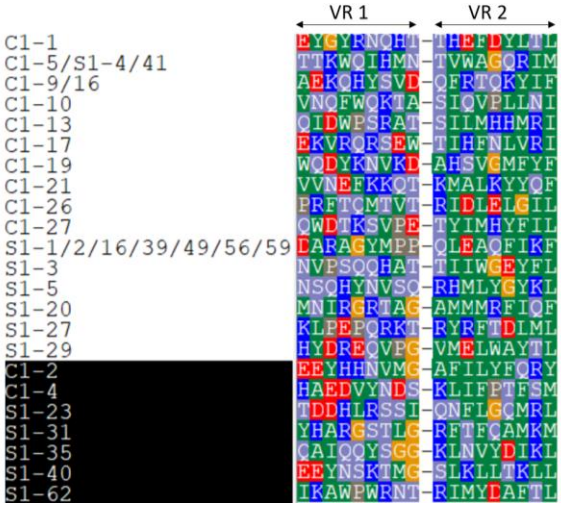

Figure 21: Variable region sequences of Affimer reagents selected following phage ELISA from phage display 1. The sequences of the unique VRs of the 32 Affimer reagents were visualised in BioEdit. Amino acids are categorised by colour according to their properties; green for hydrophobic side chains, grey for uncharged side chains, red for negatively charged side chains, blue for positively charged side chains, orange for glycine, and brown for proline. Affimer reagent names highlighted in black correspond to Affimer reagents determined to be SOS2^{cat} selective during phage ELISA.

3.7 Affimer reagents isolated in phage display 1 did not inhibit SOS1^{cat} or SOS2^{cat} catalysed nucleotide exchange

Following the isolation of 23 unique SOS2^{cat} binding Affimer reagents, they were tested in the SOS2^{cat} and SOS1^{cat} catalysed nucleotide exchange assays to determine whether they inhibit SOS2^{cat} and/or SOS1^{cat}.

The 23 unique pDHIS phagemids were prepared and transformed into JM83 cells, colonies picked and grown in 50 mL cultures to produce protein (section 2.13). Proteins were purified using magnetic nickel beads on the KingFisher Flex. To confirm the proteins were being produced and to check the purity, samples were collected from the elutions and run on a 15% SDS-PAGE and stained with Coomassie blue (figure 22A). Bands indicating protein were present at the expected molecular weight of approximately 12 kDa (indicated by an arrow). Purified proteins were dialysed into nucleotide exchange buffer and the Affimer proteins were tested in both the SOS1^{cat} and SOS2^{cat} catalysed nucleotide exchange assays (section 2.7.6). Due to the low concentration of Affimer produced via JM83 expression, the SOS2^{cat} concentration in the nucleotide exchange assay was halved to 0.25 µM, the same concentration of SOS1^{cat}, in order to keep the ratio of Affimer to SOS constant for both SOS isoforms.

No Affimer reagents inhibited SOS1^{cat} or SOS2^{cat} catalysed nucleotide exchange (figures 22B and 22C). Affimers C1-13 and C1-26 showed potential inhibition via slightly decreased initial rates with SOS2^{cat} and SOS1^{cat} respectively, which were statistically significant, however these decreases are minimal and would have no further use. Other Affimer reagents demonstrated initial rates statistically significant compared to the SOS controls, however these were faster initial rates and thus were likely caused by pipetting errors and do not demonstrate inhibition of SOS1^{cat} or SOS2^{cat}.

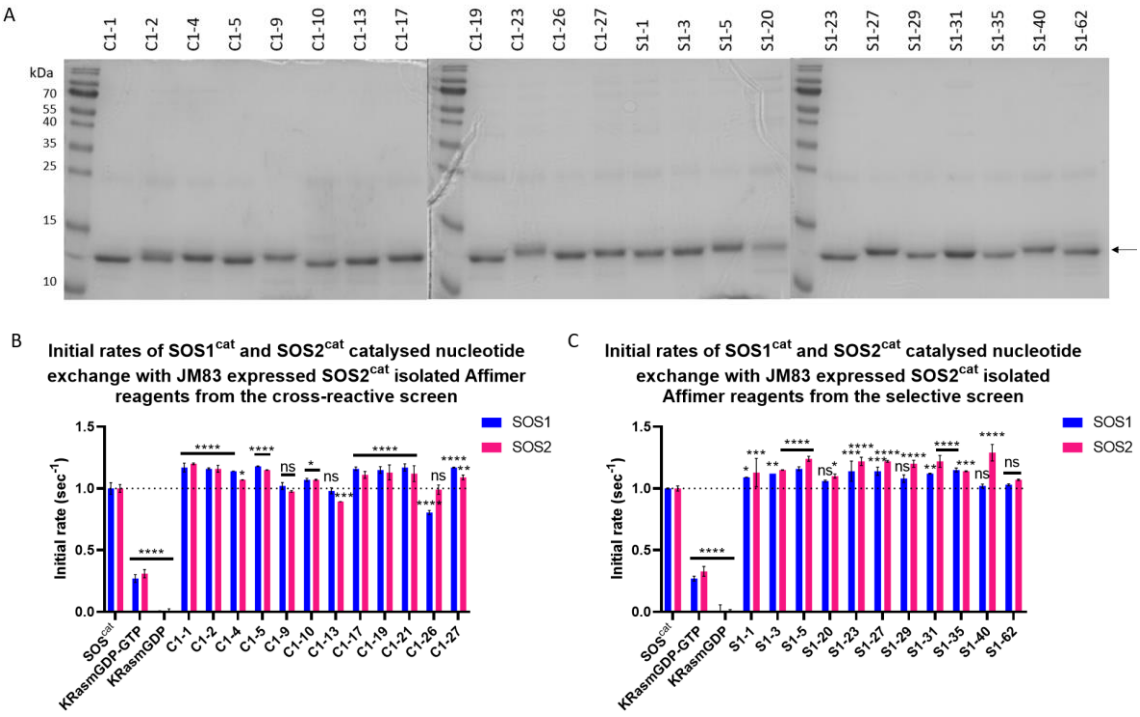

Figure 22: Production and purification of SOS2^{cat} isolated Affimer reagents, which showed lack of inhibition of SOS1^{cat} and SOS2^{cat} catalysed nucleotide exchange. (A) Following production of Affimer proteins in JM83 cells, elution samples were taken which were run on a 15% SDS-PAGE and stained with Coomassie blue. JM83 expressed Affimer proteins at 5 µM from the (B) cross-reactive screen and (C) the selective screen were assayed against 0.25 µM SOS1^{cat} or SOS2^{cat} catalysed nucleotide exchange. KRasmGDP-GTP demonstrates the initial rate of intrinsic nucleotide exchange in the absence of SOS and inhibitors. Initial rates of nucleotide exchange were normalised to SOS and KRasmGDP controls. Dashed line denotes initial rate of normalised SOS^{cat} control. Results represent one biological repeat (n = 1). Error bars are ± SD. $p > 0.05$ (ns), $p < 0.05$ (*), $p < 0.005$ (**), $p < 0.001$ (***), $p < 0.0001$ (****).

However, since no positive control was tested, the results needed to be validated. Therefore, JM83 protein production and purification of the seven selective Affimer reagents was repeated alongside Affimer s18 as a positive control. Only selective Affimer reagents were repeated since cross-reactive Affimer reagents have already been identified, such as Affimer s18, making selective Affimer reagents of more interest. Following purification, samples from the elution were collected and run on a 15% SDS-PAGE and stained with Coomassie blue (figure 23A). Bands indicating protein were present at the expected molecular weight of approximately 12 kDa (indicated by an arrow). These purified proteins were dialysed into nucleotide exchange buffer and the Affimer proteins were tested in the SOS1^{cat} and SOS2^{cat} catalysed nucleotide exchange assays (figure 23B). These results validated the previous results (figure 22B), demonstrating that the isolated Affimer reagents did not inhibit SOS2^{cat} or SOS1^{cat}. The initial rates with the SOS2^{cat} selective Affimer reagents were not statistically significant compared to the SOS controls. The positive control, Affimer s18, demonstrated inhibition of both SOS1^{cat} and SOS2^{cat}, with greater inhibition of SOS1^{cat}.

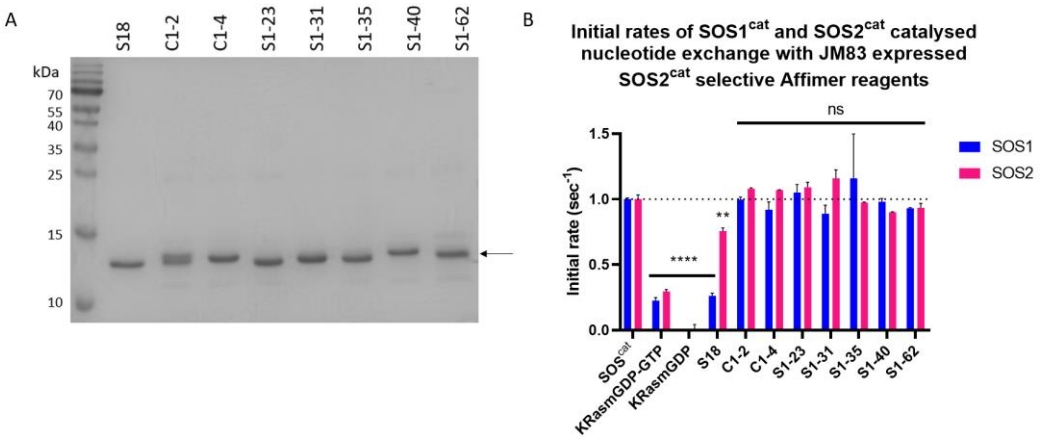

Figure 23: Repeated production and purification of SOS2^{cat} Affimer reagents, which show lack of inhibition of SOS1^{cat} and SOS2^{cat} catalysed nucleotide exchange, alongside cross-reactive Affimer s18 as a positive control. (A) Following repeat production of Affimer proteins, including Affimer s18 as a positive control, in JM83 cells, elution samples were taken which were run on a 15% SDS-PAGE and stained with Coomassie blue. (B) JM83 expressed Affimer proteins, including Affimer s18 as a positive control, at 5 µM were assayed against 0.25 µM SOS1^{cat} or SOS2^{cat} catalysed nucleotide exchange. KRasmGDP-GTP demonstrates the initial rate of intrinsic nucleotide exchange in the absence of SOS and inhibitors. Initial rates of nucleotide exchange were normalised to SOS and KRasmGDP controls. Dashed line denotes initial rate of normalised SOS^{cat} control. Results represent one biological repeat (n = 1). Error bars are ± SD. $p > 0.05$ (ns), $p < 0.005$ (**), $p < 0.0001$ (****).

3.8 Phage display 2: Isolation of SOS2^{cat} binding Affimer reagents with HPDP biotinylated SOS2^{cat} and SOS1^{cat}

Since no SOS2^{cat} inhibitors were isolated, a second phage display screen was undertaken with changes to the buffer used and method of biotinylation. PBST was switched for nucleotide exchange buffer to make screening conditions similar to the inhibition testing conditions. An alternative method of biotinylation is using EZ-link HPDP biotin which labels sulfhydryls (-SH), such as the side chain of cysteine residues. The catalytic domains of both SOS2 and SOS1 contain 5 cysteine residues each.

Purified SOS1^{cat} and SOS2^{cat} were biotinylated and then characterised before use (section 2.9) (figure 24). Due to the potential that disulphide bonds may form, half of the SOS2^{cat} protein was incubated in TCEP resin prior to biotinylation to reduce any disulphide bonds. However, incubation in TCEP resin resulted in low protein concentrations of SOS2-B (figure 24B). Therefore, although SOS2-B incubated in TCEP resin was biotinylated, as shown via ELISA, the low protein concentration meant it was unusable for phage display screening. Therefore, SOS1^{cat} and SOS2^{cat} were biotinylated without reduction of any potential disulphide bonds. SOS1-B and SOS2-B were at similar protein concentrations and both showed clear biotinylation via ELISA. Western blot analysis was performed in the absence of β-mercaptoethanol to prevent reduction of disulphide bonds which would have reduced the bond between the protein and HPDP biotin. Both SOS1^{cat} and SOS2^{cat} were clearly biotinylated, with a positive control of NHS biotinylated SOS2^{cat}. The biotinylated form of the proteins also demonstrated high levels of protein activity in the nucleotide exchange assay, similar to the unbiotinylated forms, even though there is significant difference. However, the initial rates were above the rate of intrinsic nucleotide exchange, demonstrating that SOS1-B and SOS2-B are still active. Therefore, EZ-link HPDP biotinylated SOS1^{cat} and SOS2^{cat} were used for the second phage display screens.

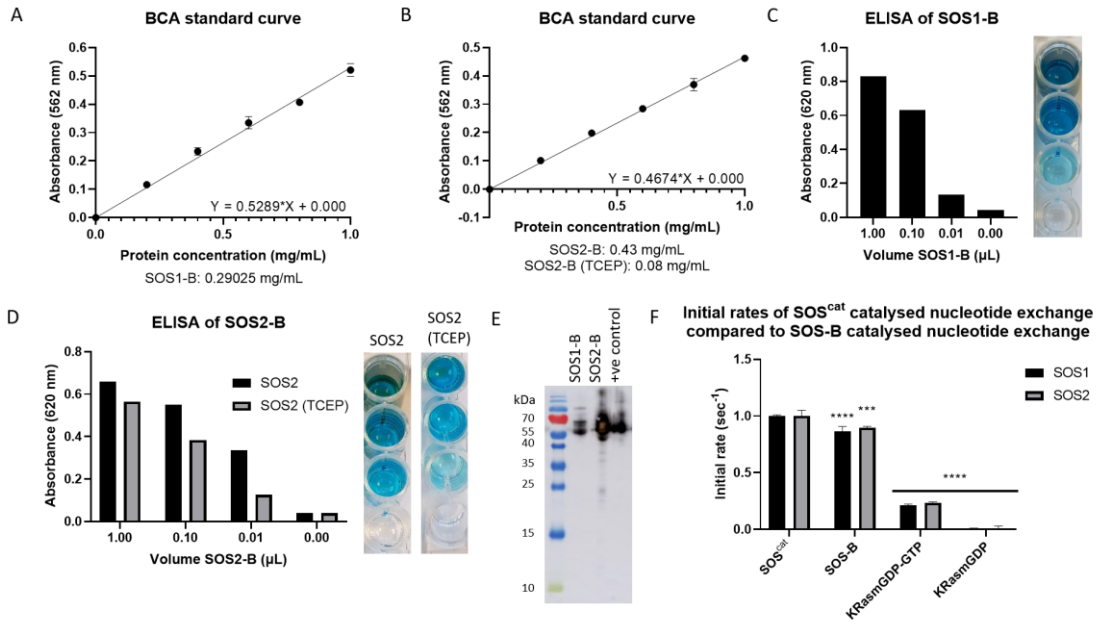

Figure 24: Characterisation of HPDP biotinylated SOS1^{cat} and SOS2^{cat}. Biotinylated (A) SOS1^{cat} and (B) SOS2^{cat} protein concentration was determined using a BCA protein assay kit, with standards and protein samples measured at 562 nm. Error bars are ± SD. Biotinylation of (C) SOS1^{cat} and (D) SOS2^{cat}, with and without TCEP treatment, was validated via ELISAs at varying protein volumes, with A_{620} measured and photograph taken. (E) Biotinylation of SOS1^{cat} and SOS2^{cat} was further validated via western blot analysis probed with Streptavidin-HRP. Samples were not reduced with β-mercaptoethanol and NHS biotinylated SOS2^{cat} was used as a positive control. (F) Initial rates of nucleotide exchange of SOS1-B and SOS2-B was compared to the unbiotinylated form. KRasmGDP-GTP demonstrates the initial rate of intrinsic nucleotide exchange in the absence of SOS and inhibitors. Initial rates of nucleotide exchange were normalised to the corresponding SOS isoform and KRasmGDP controls. Results represent one biological repeat (n = 1). Error bars are ± SD. $p < 0.001$ (***), $p < 0.0001$ (****).

Using the HPDP biotinylated SOS2^{cat} and SOS1^{cat}, two phage display screens were carried out side-by-side, selective and cross-reactive, in nucleotide exchange buffer as described for the first phage display screens (section 3.6) and in section 2.10. Following the third round of panning, ER2738 *E. coli* cells were infected with phage and a range of volumes plated onto LB-carb plates. Following overnight incubation, the number of colonies on plates with 10 µL phage-infected ER2738 *E. coli* cells were counted, estimated or calculated from 1 µL phage (table 11).

Both screens contained one colony on the blank plates, which is ideal as it indicates that few Affimer reagents bound the plastic wells rather than the target proteins. Both screens contained a large number of colonies on the SOS2^{cat} plates and fewer on the SOS1^{cat} plates. This is ideal for

the cross-reactive screen, as it indicates that some of the SOS2^{cat} binders isolated in panning rounds 1 and 2 also bind SOS1^{cat}. However it is less ideal for the selective screen as SOS1^{cat} binders should have been deselected during the pre-panning rounds 2 and 3. Nonetheless, colonies from each screen were picked for phage ELISA; 96 from the SOS2^{cat} plates of the selective screen and 96 from the SOS1^{cat} plates of the cross-reactive screen.

Screen	Number of colonies on 10 µL plate		
	SOS2^{cat}	SOS1^{cat}	Blank
Selective	**16,600 (^)**	1,500 (~)	1
Cross-reactive	20,000 (~)	**2,300 (^)**	1

Table 11: Number of colonies present on 10 µL LB-carb plates following phage display 2. Following panning round 3, phage bound to the SOS2^{cat}, SOS1^{cat} and blank panning wells were infected into ER2738 *E. coli* cells. Phage-infected cells were plated onto LB-carb plates at a range of volumes, which were incubated overnight at 37°C and the number of colonies on the 10 µL plate counted, calculated from the 1 µL plate as denoted by ^ symbol, or estimated as denoted by ~ symbol. Bold denotes the plates from which colonies were picked for phage ELISA.

The colonies picked were tested in phage ELISA against SOS2^{cat}, SOS1^{cat} and blank control (section 2.11). The colonies were named and numbered, with S2 denoting Affimer reagents picked from the selective screen, while C2 denoting those from the cross-reactive screen. From the 192 colonies picked and tested in phage ELISA (figure 25), only 11 bound the blank well, defined as A_{620} below 0.05. Therefore, only the 35 categorised as SOS2^{cat} selective binders were taken forward for sequencing, defined as A_{620} below 0.1 for SOS1^{cat}.

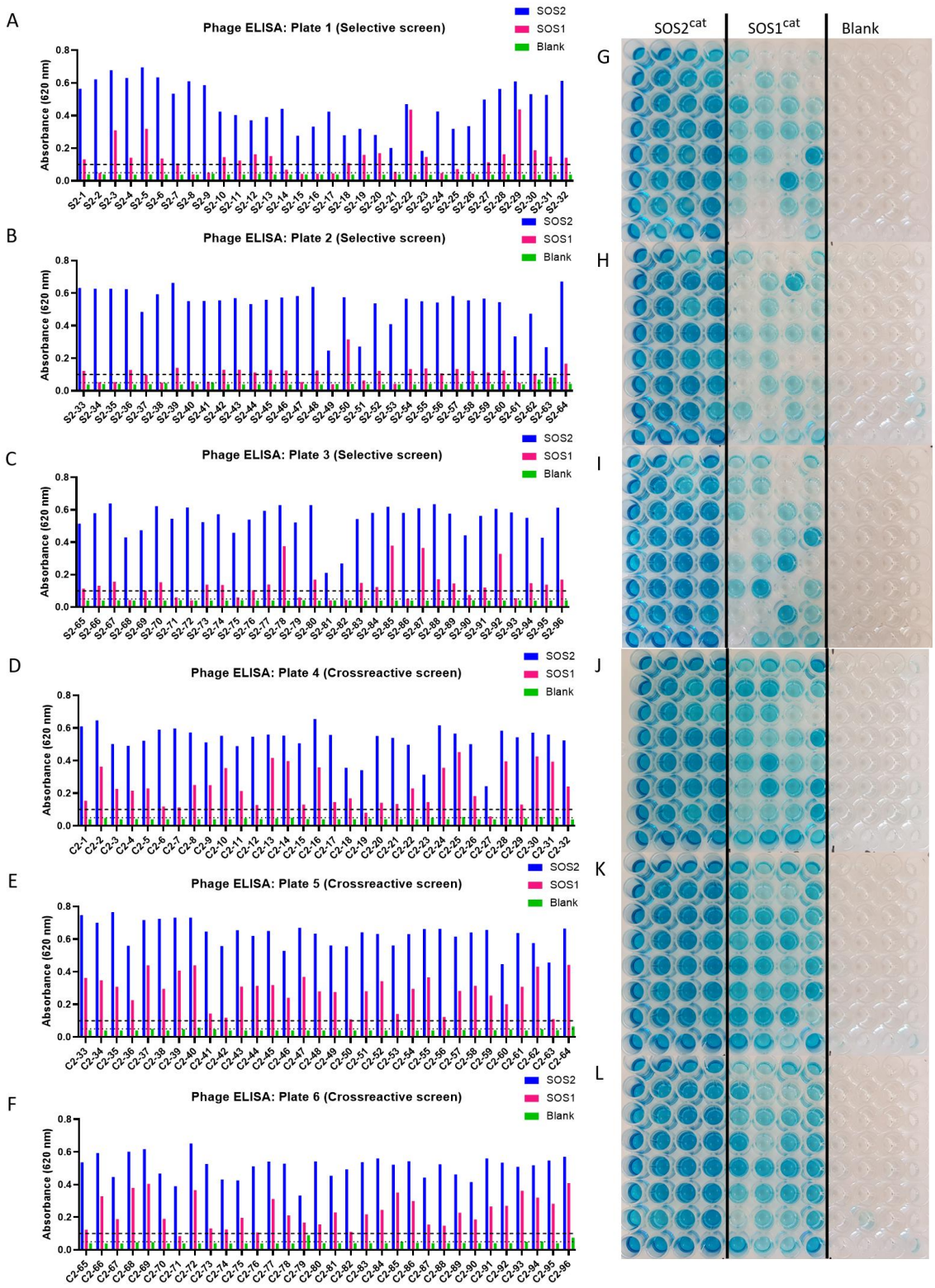

Figure 25: Phage ELISA from phage display 2. From the phage-infected ER2738 *E. coli* cells plated onto LB-carb plates, 192 colonies were picked, and the phage amplified; 96 from the selective screen and 96 from the cross-reactive screen. These were then tested in phage ELISA against SOS2^{cat}, SOS1^{cat} and a blank well. (A-C) Phage ELISA plates were measured at A_{620}. Raw results were graphed dotted line A_{620} = 0.05 denoting background levels, dashed line denoting A_{620} = 0.1 for highest value of SOS1^{cat} for SOS2^{cat} selective Affimer reagents taken forward. (D-F) These phage ELISA plates were also photographed for visualisation.

From the 35 SOS2^{cat} selective Affimer reagents sequenced using the universal M13R primer (section 2.12), only Affimer C2-19 did not prime, with the other 34 Affimer reagents giving 19 unique sequences (figure 26). While most contained 9 residues in VR 1 and 9 residues in VR 2, Affimer S2-75 contains 10 residues in VR 1 and 9 residues in VR 2. This is uncommon but can happen due to the random generation of the Affimer libraries.

There are no clear similarities between the 19 unique sequences, except they all contain hydrophobic residues in position 2.9 and the majority contain hydrophobic residues in positions 2.2, 2.4 and 2.7. This is similar to the Affimer reagents isolated in the first phage display screens; however, there are no identical sequences to the first phage display or no similarities with Affimer s18, except hydrophobic residues in positions 2.4, 2.7 and 2.9.

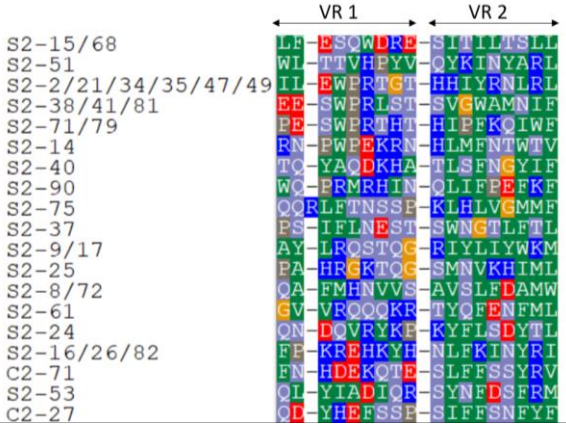

Figure 26: Variable region sequences of SOS2^{cat} selective Affimer reagents selected following phage ELISA from phage display 2. The sequences of the unique VRs of the 34 Affimer reagents were visualised in BioEdit. Amino acids are categorised by colour according to their properties; green for hydrophobic side chains, grey for uncharged side chains, red for negatively charged side chains, blue for positively charged side chains, orange for Glycine, and brown for Proline.

The next step for this project is to produce these 19 unique SOS2^{cat} selective Affimer reagents via JM83 expression and test them in the SOS1^{cat} and SOS2^{cat} catalysed nucleotide exchange assays to determine whether they inhibit SOS2^{cat} and/or SOS1^{cat}. Since these Affimer reagents showed selective characteristics in the phage ELISA, they should not inhibit SOS1^{cat}, but may inhibit SOS2^{cat}. If SOS2^{cat} selective inhibitors are isolated, they could be used to investigate the effects of inhibiting SOS2 in mammalian cells assays, such as by looking at the effects on downstream signalling of the MAPK/ERK and PI3K/Akt pathways. Additionally, previously

isolated and characterised SOS1^{cat} specific and cross-reactive inhibitors could also be used to interrogate the role of SOS2 in Ras mediated cancer signalling.

4. Discussion

4.1 Affimer s18

This project has successfully further characterised Affimer s18, a SOS1/SOS2 cross-reactive Affimer inhibitor, as well as isolating $SOS2^{cat}$ binders which have the potential for selective inhibition of $SOS2^{cat}$.

To determine the potency of the cross-reactive Affimer s18 for $SOS1^{cat}$, an IC_{50} curve was carried out of the $SOS1^{cat}$ catalysed nucleotide exchange assay with varying concentrations of Affimer s18. This gave an IC_{50} value of 176.2 nM ± 9.92 for Affimer s18 against $SOS1^{cat}$. A previously identified SOS1 inhibitor, compound BAY-293, was shown to inhibit the G12C KRas-$SOS1^{cat}$ interaction with an IC_{50} of 21 nM [36]. While both values are in the nanomolar range, the IC_{50} values are not comparable due to assay differences; with the interaction assay looking at the inhibition of the interaction of SOS1 and KRas rather than the inhibition of nucleotide exchange and thus activation of KRas. However, it demonstrates that Affimer s18 is a potent inhibitor of $SOS1^{cat}$.

At the higher concentrations of Affimer s18, the initial rates of $SOS1^{cat}$ catalysed nucleotide exchange are inhibited to levels of intrinsic nucleotide exchange. Thus, Affimer s18 can completely inhibit $SOS1^{cat}$. Affimer s18 was also shown to completely inhibit $SOS2^{cat}$ at a high Affimer s18 concentration. It would be interesting to further explore the inhibition of $SOS2^{cat}$ by Affimer s18 by determining its potency. While this would not be directly comparable to the IC_{50} value obtained against $SOS1^{cat}$, since the concentration of $SOS2^{cat}$ is double that of $SOS1^{cat}$ in the respective nucleotide exchange assays, it would indicate whether Affimer s18 inhibits both isoforms to a similar extent. For example, if the IC_{50} value for Affimer s18 against $SOS2^{cat}$ was double that of Affimer s18 against $SOS1^{cat}$, then it could be assumed that Affimer s18 inhibits both isoforms to the same extent. This could also be used to compare the potency of cross-reactive Affimer reagents, such as Affimer s18, with $SOS2^{cat}$ selective Affimer inhibitors potentially isolated in phage display 2.

Alanine scanning of Affimer s18 identified five residues important for inhibiting $SOS1^{cat}$. These residues are present in both VRs of Affimer s18, indicating that both VRs are important for either the binding to or the inhibition of $SOS1^{cat}$. However, with only two repeats for VR 1 mutants and a single repeat for VR 2 mutants, the data needs to be repeated to three biological repeats per VR to perform statistical analysis and validate the results.

While alanine scanning allows these important residues to be identified, it does not help identify the location at which Affimer s18 binds to $SOS1^{cat}$. In order to determine the location of binding

of Affimer s18 to SOS1^{cat}, structural analysis needs to be carried out. However, so far X-ray crystallography has been unsuccessful. Thus, it cannot be determined whether the location at which Affimer s18 binds SOS1^{cat} is conserved in SOS2^{cat}. However, since Affimer s18 has been shown to inhibit SOS2^{cat} as well as SOS1^{cat}, the location could be expected to be conserved. It would therefore be interesting to perform alanine scanning with the SOS2^{cat} catalysed nucleotide exchange assay. This could be used to determine whether the same residues are important for binding and inhibiting both isoforms of SOS, and thus whether Affimer s18 is likely to be binding to SOS1^{cat} and SOS2^{cat} in the same manner to a conserved region or in a slightly different way, for example with different important residues, which would also have an effect on potency.

4.2 Biochemical nucleotide exchange assays

KRas nucleotide exchange assays catalysed by SOS1^{cat} or SOS2^{cat} were used to determine the inhibition of SOS1^{cat} and SOS2^{cat} by Affimer reagents. KRas is loaded with mGDP which is exchanged for GTP, intrinsically and catalysed by SOS. mGDP allows the rate of exchange to be monitored due to its fluorescent label, N-Methylanthraniloyl, which dramatically loses its fluorescent signal when dissociated from a GTPase [82]. Additionally, its small size means it is unlikely to interfere with the protein-nucleotide interaction [82].

The SOS2^{cat} catalysed nucleotide exchange assay was optimised for use following the optimisation of SOS2^{cat} protein production. For the SOS2^{cat} catalysed nucleotide exchange assay, the concentration of SOS2^{cat} is double that of SOS1^{cat} in the SOS1^{cat} catalysed nucleotide exchange assay. This implies that SOS2^{cat} is half as active in catalysing nucleotide exchange of purified proteins. This difference is also observed in other published assays, such as a G12C KRas-SOS^{cat} interaction assay where the final concentration of SOS1^{cat} is 10 nM, while that of SOS2^{cat} is 20 nM, with no change in KRas concentration [36].

It is important to note that the nucleotide exchange assays used KRas. The other two isoforms of Ras, HRas and NRas, may therefore require different concentrations of SOS1^{cat} or SOS2^{cat} to obtain the similar initial rates of nucleotide exchange. By testing Affimer reagents against SOS in nucleotide exchange assays containing the different isoforms of Ras, it can be determined whether the Affimer inhibitors of SOS affect the activation of the three Ras isoforms differently. Additionally, this could further elicit which isoform of Ras is most effectively catalysed by SOS2^{cat}.

4.3 Phage display isolated SOS2^{cat} binders

Following phage display 1, where SOS2^{cat} and SOS1^{cat} were biotinylated on the lysine residues and the screen was carried out in PBST, the phage ELISA showed a high proportion of isolated

Affimer reagents which bound the blank wells. This was likely caused by a large number of hydrophobic residues or arginine repeats in the VRs. Hydrophobic residues include alanine, valine, isoleucine, methionine, phenylalanine, tyrosine and tryptophan. This occurs as the libraries used are randomly generated. These Affimer reagents would have likely bound the panning well plastic, not the $SOS2^{cat}$ protein, in the first round of panning and thus were amplified, leading to an increased number of hydrophobic or arginine repeat containing Affimer reagents in the second panning round and further amplified for the third panning round.

While this indicated the screen was not the most successful, Affimer reagents which did not bind the blank wells but bound $SOS2^{cat}$ were still isolated successfully. These Affimer reagents were produced, purified and tested in the $SOS1^{cat}$ and $SOS2^{cat}$ catalysed nucleotide exchange assays. They showed no inhibitory properties of either $SOS1^{cat}$ or $SOS2^{cat}$. They were probably not binding in the active or allosteric sites, but rather elsewhere on SOS which does not affect KRas binding and thus would not inhibit SOS. Therefore, a second phage display was carried out to try to isolate $SOS2^{cat}$ binders which also inhibit.

Following phage display 2, where $SOS2^{cat}$ and $SOS1^{cat}$ were biotinylated on the cysteine residues and the screen was carried out in nucleotide exchange buffer, the phage ELISA showed the majority of isolated Affimer reagents did not bind the blank wells. This indicated a more successful screen, however, due to the high number of isolated Affimer reagents, not all could feasibly be sequenced and tested in the nucleotide exchange assays. Therefore, only the $SOS2^{cat}$ selective Affimer reagents were taken forward for sequencing and testing, since cross-reactive Affimer reagents have previously been isolated and characterised, including Affimer s18.

The Affimer reagents obtained in phage display 2 were different compared to phage display 1; however, the majority of Affimer reagents isolated in both phage displays displayed a similar motif of hydrophobic residues in VR positions 2.2, 2.4, 2.7 and 2.9. Since this is a prominent motif, it is likely these residues are important for binding to $SOS2^{cat}$. Interestingly, the cross-reactive inhibitor Affimer s18 also contains hydrophobic residues in positions 2.4, 2.7 and 2.9, as well as 1.5, 1.8 and 2.8, with the tyrosine in position 2.4 was shown to be important for inhibiting $SOS1^{cat}$.

The next step is to test the second set of $SOS2^{cat}$ selective Affimer reagents in both the $SOS2^{cat}$ and $SOS1^{cat}$ catalysed nucleotide exchange assays to determine whether they inhibit $SOS2^{cat}$ and to show they do not inhibit $SOS1^{cat}$, since they showed no binding in the phage ELISA.

It is important to note that Affimer reagents were isolated against the catalytic domain of SOS2. Inhibitors may bind in any location on the catalytic domain which may not be accessible in the full length of SOS2 found in cells. Therefore, SOS2 inhibitors of nucleotide exchange in the

biochemical assays still need to be tested in mammalian cell assays to confirm they are effective against SOS2.

4.4 Continuation of the project

After the Affimer reagents isolated in phage display 2 are characterised, isolated inhibitors can be taken forward both for further biochemical characterisation, such as alanine scanning as discussed above, and for testing in mammalian cell assays to determine their ability to inhibit full length SOS2 and to further elicit the role of SOS2 in Ras mediated cancer signalling.

Mammalian cells assays could look at the downstream signalling effects of inhibiting SOS1 and SOS2 with Affimer reagents, focussing on the phosphorylation and activation of ERK and Akt, downstream signalling proteins in the MAPK/ERK and PI3K/Akt pathways respectively. This may be measured with immunofluorescence imaging or pull-down assays following transfection of GFP labelled Affimer reagents. Not only would this look at the effects of SOS2 on downstream signalling, it would also indicate whether the Affimer reagents are able to inhibit full length SOS2.

In MEFs harbouring mutant Ras, knock-out of SOS2 demonstrated decreased phosphorylation of Akt, with no significant decrease detected in levels of ERK phosphorylation [68]. Therefore, it can be hypothesised that inhibiting SOS2 with $SOS2^{cat}$ selective Affimer reagents would have a greater effect on the levels of phosphorylated Akt than that of ERK. These levels can be compared to the inhibition of SOS1 alone and inhibition of both SOS isoforms. Additionally, the effects of inhibiting SOS2 in cells harbouring mutations in different Ras isoforms and in cells without Ras mutations could be investigated. This would identify the mutant Ras isoforms most dependent on SOS2 and the differences of SOS2 importance in cancer and non-cancer cells.

Knock-out of SOS2 in MEFs showed SOS2 not to be a critical mediator of cell proliferation, but rather for cellular transformation, particularly for cells harbouring mutated KRas [68, 69]. Therefore, it can be hypothesised that inhibition of SOS2 with SOS2 selective Affimer reagents would have limited effects on cell growth but should reduce transformation, particularly in cancer cell lines with high levels of mutant KRas. A mixture of selective and cross-reactive Affimer inhibitors of SOS1 and SOS2 could be used to determine which isoform, or whether both isoforms, should be inhibited in order to reduce cell transformation in an array of cancer cell lines harbouring different Ras mutations. This could be achieved by looking at spheroid growth. This would validate the role of SOS2 in cellular transformation and further identify its role in Ras mediated signalling. However, the transient nature of transfection would mean that growth assay would require more stable transfection methods, such as the use of lentiviral expression vectors to produce stable cell lines expressing Affimer reagent.

Putting different mammalian cell assay results together will allow the role and importance of SOS2 in Ras mediated cancer signalling to be further elicited and thus determine whether there are potential therapeutic benefits to inhibiting SOS2. Additionally, SOS2 Affimer inhibitors could also be tested with Ras Affimer inhibitors to determine the potential benefits of co-inhibition.

4.5 Conclusion

The previously isolated SOS1/SOS2 cross-reactive Affimer s18 was further characterised to demonstrate that it inhibits $SOS1^{cat}$ with an IC_{50} of 176.2 nM and has the ability to inhibit $SOS2^{cat}$. Additionally, five residues were identified via alanine scanning which proved important for the inhibition of $SOS1^{cat}$. Furthermore, Affimer reagents which bind $SOS2^{cat}$, selectively and cross-reactively, were isolated in two phage display screens. From the first screen, no inhibitors were isolated, while $SOS2^{cat}$ selective Affimer reagents from the second screen still need to be characterised. Once characterised for inhibition, selective inhibitors of $SOS2^{cat}$ can be further characterised in biochemical assays and tested in mammalian cell assays to further elicit the role of SOS2 in Ras mediated cancer signalling.

References

1. Sever, R. and J.S. Brugge, *Signal transduction in cancer.* Cold Spring Harb Perspect Med, 2015. **5**(4).
2. Prior, I.A., P.D. Lewis, and C. Mattos, *A comprehensive survey of Ras mutations in cancer.* Cancer Res, 2012. **72**(10): p. 2457-67.
3. Qi, M. and E.A. Elion, *MAP kinase pathways.* J Cell Sci, 2005. **118**(Pt 16): p. 3569-72.
4. Boni-Schnetzler, M. and P.F. Pilch, *Mechanism of epidermal growth factor receptor autophosphorylation and high-affinity binding.* Proc Natl Acad Sci U S A, 1987. **84**(22): p. 7832-6.
5. Lemmon, M.A. and J. Schlessinger, *Cell signaling by receptor tyrosine kinases.* Cell, 2010. **141**(7): p. 1117-34.
6. Lowenstein, E.J., et al., *The SH2 and SH3 domain-containing protein GRB2 links receptor tyrosine kinases to ras signaling.* Cell, 1992. **70**(3): p. 431-42.
7. Li, N., et al., *Guanine-nucleotide-releasing factor hSos1 binds to Grb2 and links receptor tyrosine kinases to Ras signalling.* Nature, 1993. **363**(6424): p. 85-8.
8. Rojas, J.M., J.L. Oliva, and E. Santos, *Mammalian son of sevenless Guanine nucleotide exchange factors: old concepts and new perspectives.* Genes Cancer, 2011. **2**(3): p. 298-305.
9. Zhou, Y., et al., *Lipid-Sorting Specificity Encoded in K-Ras Membrane Anchor Regulates Signal Output.* Cell, 2017. **168**(1-2): p. 239-251.e16.
10. Chong, H., H.G. Vikis, and K.L. Guan, *Mechanisms of regulating the Raf kinase family.* Cell Signal, 2003. **15**(5): p. 463-9.
11. Alessi, D.R., et al., *Identification of the sites in MAP kinase kinase-1 phosphorylated by p74raf-1.* Embo j, 1994. **13**(7): p. 1610-9.
12. Ferrell, J.E., Jr. and R.R. Bhatt, *Mechanistic studies of the dual phosphorylation of mitogen-activated protein kinase.* J Biol Chem, 1997. **272**(30): p. 19008-16.
13. Anderson, N.G., et al., *Requirement for integration of signals from two distinct phosphorylation pathways for activation of MAP kinase.* Nature, 1990. **343**(6259): p. 651-3.
14. Yoon, S. and R. Seger, *The extracellular signal-regulated kinase: multiple substrates regulate diverse cellular functions.* Growth Factors, 2006. **24**(1): p. 21-44.
15. John, J., et al., *Kinetics of interaction of nucleotides with nucleotide-free H-ras p21.* Biochemistry, 1990. **29**(25): p. 6058-65.

16. Gideon, P., et al., *Mutational and kinetic analyses of the GTPase-activating protein (GAP)-p21 interaction: the C-terminal domain of GAP is not sufficient for full activity.* Mol Cell Biol, 1992. **12**(5): p. 2050-6.
17. Scheffzek, K., M.R. Ahmadian, and A. Wittinghofer, *GTPase-activating proteins: helping hands to complement an active site.* Trends Biochem Sci, 1998. **23**(7): p. 257-62.
18. Manning, B.D. and L.C. Cantley, *AKT/PKB signaling: navigating downstream.* Cell, 2007. **129**(7): p. 1261-74.
19. Castellano, E. and J. Downward, *RAS Interaction with PI3K: More Than Just Another Effector Pathway.* Genes Cancer, 2011. **2**(3): p. 261-74.
20. Domchek, S.M., et al., *Inhibition of SH2 domain/phosphoprotein association by a nonhydrolyzable phosphonopeptide.* Biochemistry, 1992. **31**(41): p. 9865-70.
21. Cuevas, B.D., et al., *Tyrosine phosphorylation of p85 relieves its inhibitory activity on phosphatidylinositol 3-kinase.* J Biol Chem, 2001. **276**(29): p. 27455-61.
22. Zhang, M., H. Jang, and R. Nussinov, *The structural basis for Ras activation of PI3Kalpha lipid kinase.* Phys Chem Chem Phys, 2019. **21**(22): p. 12021-12028.
23. Alessi, D.R., et al., *Mechanism of activation of protein kinase B by insulin and IGF-1.* Embo j, 1996. **15**(23): p. 6541-51.
24. Alessi, D.R., et al., *Characterization of a 3-phosphoinositide-dependent protein kinase which phosphorylates and activates protein kinase Balpha.* Curr Biol, 1997. **7**(4): p. 261-9.
25. Liao, Y. and M.C. Hung, *Physiological regulation of Akt activity and stability.* Am J Transl Res, 2010. **2**(1): p. 19-42.
26. Voice, J.K., et al., *Four human ras homologs differ in their abilities to activate Raf-1, induce transformation, and stimulate cell motility.* J Biol Chem, 1999. **274**(24): p. 17164-70.
27. Cox, A.D. and C.J. Der, *Ras history: The saga continues.* Small GTPases, 2010. **1**(1): p. 2-27.
28. Cox, A.D., et al., *Drugging the undruggable RAS: Mission possible?* Nat Rev Drug Discov, 2014. **13**(11): p. 828-51.
29. Hanahan, D. and R.A. Weinberg, *The hallmarks of cancer.* Cell, 2000. **100**(1): p. 57-70.
30. Muñoz-Maldonado, C., Y. Zimmer, and M. Medová, *A Comparative Analysis of Individual RAS Mutations in Cancer Biology.* Front Oncol, 2019. **9**: p. 1088.
31. Jeng, H.H., L.J. Taylor, and D. Bar-Sagi, *Sos-mediated cross-activation of wild-type Ras by oncogenic Ras is essential for tumorigenesis.* Nat Commun, 2012. **3**: p. 1168.
32. Patgiri, A., et al., *An orthosteric inhibitor of the Ras-Sos interaction.* Nat Chem Biol, 2011. **7**(9): p. 585-7.

33. Canon, J., et al., *The clinical KRAS(G12C) inhibitor AMG 510 drives anti-tumour immunity.* Nature, 2019. **575**(7781): p. 217-223.
34. Patricelli, M.P., et al., *Selective Inhibition of Oncogenic KRAS Output with Small Molecules Targeting the Inactive State.* Cancer Discov, 2016. **6**(3): p. 316-29.
35. Janes, M.R., et al., *Targeting KRAS Mutant Cancers with a Covalent G12C-Specific Inhibitor.* Cell, 2018. **172**(3): p. 578-589.e17.
36. Hillig, R.C., et al., *Discovery of potent SOS1 inhibitors that block RAS activation via disruption of the RAS-SOS1 interaction.* Proc Natl Acad Sci U S A, 2019. **116**(7): p. 2551-2560.
37. Jones, S., M.L. Vignais, and J.R. Broach, *The CDC25 protein of Saccharomyces cerevisiae promotes exchange of guanine nucleotides bound to ras.* Mol Cell Biol, 1991. **11**(5): p. 2641-6.
38. Bonfini, L., et al., *The Son of sevenless gene product: a putative activator of Ras.* Science, 1992. **255**(5044): p. 603-6.
39. Bowtell, D., et al., *Identification of murine homologues of the Drosophila son of sevenless gene: potential activators of ras.* Proc Natl Acad Sci U S A, 1992. **89**(14): p. 6511-5.
40. Chardin, P., et al., *Human Sos1: a guanine nucleotide exchange factor for Ras that binds to GRB2.* Science, 1993. **260**(5112): p. 1338-43.
41. Chardin, P. and M.G. Mattei, *Chromosomal localization of two genes encoding human ras exchange factors: SOS1 maps to the 2p22-->p16 region and SOS2 to the 14q21-->q22 region of the human genome.* Cytogenet Cell Genet, 1994. **66**(1): p. 68-9.
42. Sondermann, H., et al., *Tandem histone folds in the structure of the N-terminal segment of the ras activator Son of Sevenless.* Structure, 2003. **11**(12): p. 1583-93.
43. Gureasko, J., et al., *Role of the histone domain in the autoinhibition and activation of the Ras activator Son of Sevenless.* Proc Natl Acad Sci U S A, 2010. **107**(8): p. 3430-5.
44. Chen, R.H., S. Corbalan-Garcia, and D. Bar-Sagi, *The role of the PH domain in the signal-dependent membrane targeting of Sos.* Embo j, 1997. **16**(6): p. 1351-9.
45. Zhao, C., et al., *Phospholipase D2-generated phosphatidic acid couples EGFR stimulation to Ras activation by Sos.* Nat Cell Biol, 2007. **9**(6): p. 706-12.
46. Gureasko, J., et al., *Membrane-dependent signal integration by the Ras activator Son of sevenless.* Nat Struct Mol Biol, 2008. **15**(5): p. 452-61.
47. Sondermann, H., et al., *Structural analysis of autoinhibition in the Ras activator Son of sevenless.* Cell, 2004. **119**(3): p. 393-405.
48. Nimnual, A.S., B.A. Yatsula, and D. Bar-Sagi, *Coupling of Ras and Rac guanosine triphosphatases through the Ras exchanger Sos.* Science, 1998. **279**(5350): p. 560-3.

49. Sondermann, H., et al., *Computational docking and solution x-ray scattering predict a membrane-interacting role for the histone domain of the Ras activator son of sevenless.* Proc Natl Acad Sci U S A, 2005. **102**(46): p. 16632-7.
50. Roberts, A.E., et al., *Germline gain-of-function mutations in SOS1 cause Noonan syndrome.* Nat Genet, 2007. **39**(1): p. 70-4.
51. Tartaglia, M., et al., *Gain-of-function SOS1 mutations cause a distinctive form of Noonan syndrome.* Nat Genet, 2007. **39**(1): p. 75-9.
52. Yadav, K.K. and D. Bar-Sagi, *Allosteric gating of Son of sevenless activity by the histone domain.* Proc Natl Acad Sci U S A, 2010. **107**(8): p. 3436-40.
53. Margarit, S.M., et al., *Structural evidence for feedback activation by Ras.GTP of the Ras-specific nucleotide exchange factor SOS.* Cell, 2003. **112**(5): p. 685-95.
54. Boriack-Sjodin, P.A., et al., *The structural basis of the activation of Ras by Sos.* Nature, 1998. **394**(6691): p. 337-43.
55. Egan, S.E., et al., *Association of Sos Ras exchange protein with Grb2 is implicated in tyrosine kinase signal transduction and transformation.* Nature, 1993. **363**(6424): p. 45-51.
56. Zhao, H., et al., *Insulin receptor-mediated dissociation of Grb2 from Sos involves phosphorylation of Sos by kinase(s) other than extracellular signal-regulated kinase.* J Biol Chem, 1998. **273**(20): p. 12061-7.
57. Lee, Y.K., et al., *Mechanism of SOS PR-domain autoinhibition revealed by single-molecule assays on native protein from lysate.* Nat Commun, 2017. **8**: p. 15061.
58. McDonald, C.B., et al., *Structural landscape of the proline-rich domain of Sos1 nucleotide exchange factor.* Biophys Chem, 2013. **175-176**: p. 54-62.
59. Guerrero, C., et al., *Expression of alternative forms of Ras exchange factors GRF and SOS1 in different human tissues and cell lines.* Oncogene, 1996. **12**(5): p. 1097-107.
60. Shi, T., et al., *Conservation of protein abundance patterns reveals the regulatory architecture of the EGFR-MAPK pathway.* Sci Signal, 2016. **9**(436): p. rs6.
61. Nielsen, K.H., et al., *The Ras-specific exchange factors mouse Sos1 (mSos1) and mSos2 are regulated differently: mSos2 contains ubiquitination signals absent in mSos1.* Mol Cell Biol, 1997. **17**(12): p. 7132-8.
62. Qian, X., et al., *The Sos1 and Sos2 Ras-specific exchange factors: differences in placental expression and signaling properties.* Embo j, 2000. **19**(4): p. 642-54.
63. Yang, S.S., L. Van Aelst, and D. Bar-Sagi, *Differential interactions of human Sos1 and Sos2 with Grb2.* J Biol Chem, 1995. **270**(31): p. 18212-5.

64. Corbalan-Garcia, S., et al., *Identification of the mitogen-activated protein kinase phosphorylation sites on human Sos1 that regulate interaction with Grb2.* Mol Cell Biol, 1996. **16**(10): p. 5674-82.

65. Esteban, L.M., et al., *Ras-guanine nucleotide exchange factor sos2 is dispensable for mouse growth and development.* Mol Cell Biol, 2000. **20**(17): p. 6410-3.

66. Baltanás, F.C., et al., *Functional redundancy of Sos1 and Sos2 for lymphopoiesis and organismal homeostasis and survival.* Mol Cell Biol, 2013. **33**(22): p. 4562-78.

67. Liceras-Boillos, P., et al., *Sos1 disruption impairs cellular proliferation and viability through an increase in mitochondrial oxidative stress in primary MEFs.* Oncogene, 2016. **35**(50): p. 6389-6402.

68. Sheffels, E., et al., *Oncogenic RAS isoforms show a hierarchical requirement for the guanine nucleotide exchange factor SOS2 to mediate cell transformation.* Sci Signal, 2018. **11**(546).

69. Sheffels, E., et al., *Anchorage-independent growth conditions reveal a differential SOS2 dependence for transformation and survival in RAS-mutant cancer cells.* Small GTPases, 2019: p. 1-12.

70. Hey, T., et al., *Artificial, non-antibody binding proteins for pharmaceutical and industrial applications.* Trends Biotechnol, 2005. **23**(10): p. 514-22.

71. Skrlec, K., B. Strukelj, and A. Berlec, *Non-immunoglobulin scaffolds: a focus on their targets.* Trends Biotechnol, 2015. **33**(7): p. 408-18.

72. Binz, H.K., et al., *Designing repeat proteins: well-expressed, soluble and stable proteins from combinatorial libraries of consensus ankyrin repeat proteins.* J Mol Biol, 2003. **332**(2): p. 489-503.

73. Guillard, S., et al., *Structural and functional characterization of a DARPin which inhibits Ras nucleotide exchange.* Nat Commun, 2017. **8**: p. 16111.

74. Bery, N., et al., *KRAS-specific inhibition using a DARPin binding to a site in the allosteric lobe.* Nat Commun, 2019. **10**(1): p. 2607.

75. Koide, A., et al., *The fibronectin type III domain as a scaffold for novel binding proteins.* J Mol Biol, 1998. **284**(4): p. 1141-51.

76. Spencer-Smith, R., et al., *Inhibition of RAS function through targeting an allosteric regulatory site.* Nat Chem Biol, 2017. **13**(1): p. 62-68.

77. Khan, I., R. Spencer-Smith, and J.P. O'Bryan, *Targeting the α4-α5 dimerization interface of K-RAS inhibits tumor formation in vivo.* Oncogene, 2019. **38**(16): p. 2984-2993.

78. Tiede, C., et al., *Affimer proteins are versatile and renewable affinity reagents.* Elife, 2017. **6**.

79. Tiede, C., et al., *Adhiron: a stable and versatile peptide display scaffold for molecular recognition applications.* Protein Eng Des Sel, 2014. **27**(5): p. 145-55.

80. Tang, A.A., et al., *Isolation of isoform-specific binding proteins (Affimers) by phage display using negative selection.* Sci Signal, 2017. **10**(505).

81. Haza, K.Z., et al., *RAS-inhibiting biologics identify and probe druggable pockets including an SII-α3 allosteric site.* bioRxiv, 2020: p. 2020.06.04.133728.

82. Kanie, T. and P.K. Jackson, *Guanine Nucleotide Exchange Assay Using Fluorescent MANT-GDP.* Bio Protoc, 2018. **8**(7).